THE DEVELOPMENT OF WELD THERMAL SIMULATION FOR GAS FLAME HEATING

A THESIS

Submitted in the partial fulfilment of the requirements for the degree of

Master of Engineering

in

(Mechanical)

Heat Power Engineering

of

Punjabi University, Patiala

BY

VARINDER SAHNI

Under the supervision of

Dr. GAJENDRA SINGH
Professor and Head

and

Prof. GURDIP SINGH
Reader, (Punjabi University)

Department of Mechanical Engineering
Thapar Institute of Engineering and Technology
PATIALA

MAY, 1984

CERTIFICATE

Certified that the thesis entitled, 'THE DEVELOPMENT OF WELD THERMAL SIMULATION FOR GAS FLAME HEATING', which is being submitted by Er. Varinder Sahni in partial fulfilment of the requirements for the award of the degree of MASTER OF ENGINEERING - MECHANICAL (HEAT POWER ENGG.) of Punjabi University, Patiala is a record of student's own work carried out under our supervision and guidance. The matter embodied in this thesis has not been submitted to any University or Institution for the award of any degree or diploma.

The thesis has reached the standard fulfilling the requirements of the regulations for the award of the said work.

(Dr. GAJINDRA SINGH)
Supervisor

AND

(Prof. GURDIP SINGH)
Supervisor

Dated Patiala the,
8/5 May 1984

'COUNTERSIGNED'

(Dr. Gajendra Singh)
Professor and Head,
Mechanical Engineering Deptt.,
Thapar College of Engineering,
Patiala-147001(Punjab).

(Prof. P.V. Gupta)
Dean,
Faculty of Engg.and Technology,
Punjabi University,
Patiala-147001(Punjab).

ACKNOWLEDGEMENT

The author feels pleasure in expressing his sincere and profound gratitude to Dr. Gajindra Singh, Professor and Head, Deptt. of Mechanical Engineering, Thapar College of Engineering, Patiala (Pb.) and Prof. Gurdip Singh, Reader in Deptt. of Business Management, Punjabi University, Patiala for their highly valuable guidance, at every stage of the work, without which it could not have been so successfully completed. He cannot forget the keen interest which they took in the work, right from the fabrication, experimentation on the simulator and computer programme to the thorough editing of the manuscript, often involving working at odd hours, which they did with a smile. Infact, no words are enough to record the author's semtiments of obligation towards them.

The author wish to thank Shri Vishwa Nath, Senior Instructor Workshop, for rendering assistance to the fabrication of the setup.

(VARINDER SAINI)

SYNOPSIS

Direct experimental methods to investigate changes in micro-structure and mechanical properties in Heat-Affected Zone (HAZ) of weld plate is almost impossible, due to small size of HAZ. The only alternative available is to undergo simulation studies, which can be carried out theoretically as well as experimentally. Experimental simulation can be done with the help of a open and closed loop systems. Closed loop simulation is expensive as compared to open loop simulation. With this in mind, an attempt has been made to carry out simulation studies with the help of an open loop type thermal simulator, using gas flame as an inexpensive heating source. In it emphasis is given on peak temperature and ∆t-part of the thermal cycle. These factors are mainly responsible for the phase change of steel.

Theoretical simulation is done by considering assumed linear continuous cooling time (CCT) curve and a computer programme has been developed for this analysis.

Comparison of results for hardness is made for both the techniques. Hardness trend obtained from the computer aided simulation, appears to be closely related to the experimental results, with the variations of cooling rates in the critical zone.

TABLE OF CONTENTS

NOMENCLATURE

C	=	Specific heat
d'	=	Transition plate thickness
DE	=	Density
DI	=	Diffusivity
δ	=	Thickness of plate
HI	=	Heat input
IT	=	Initial temperature ($35^{\circ}C$)
K	=	Thermal conductivity
K_o	=	Modified Bessel function of second kind and zero order
K_1	=	Modified Bessel function of second kind and order unity
n	=	Number of trials
PT	=	Peak temperature ($905.39^{\circ}C$)
q	=	Heat rate in col/min
q'	=	Heat rate per unit length
R	=	Radial coordinate
S.D.	=	Standard deviation
T	=	Temperature of interest
TC	=	Thermal conductivity
TO	=	Plate thickness (1.0 cm)
T_o	=	Initial temperature
T_a	=	Peak temperature
$\bar{T}_a$	=	Average peak temperature
t_a	=	Time taken to reach peak temperature

v	=	Velocity of electrode
X	=	Thermal diffusivity
ρ	=	Density
ξ	=	Distance of a point from centre of welding arc measured in longitudinal direction
Δt	=	Time required for cooling from $800^{\circ}C$ to $500^{\circ}C$
$\bar{\Delta t}$	=	Average value of Δt.

CHAPTER - 1

INTRODUCTION

Since last few decades, the use of steels in welding constructions such as bridges, boilers, machine tool structures etc. has become very common. Thus there has been a rapid advancement in the development of modern types of steels and the welding processes. These steels undergo drastic changes in micro-structures and mechanical properties during welding. These changes are confined to a certain area in a welded joint called Heat Affected Zone (HAZ), where temperature and deformation cycle acts during welding [1]. The information regarding these changes could be useful in predicting the weldability, stresses, strains and anticipated behaviour of these metals.

Direct experimental methods to investigate changes in micro-structures and mechanical properties in Heat Affected Zone of weld plate is almost impossible due to small size of HAZ. Apart from this, changes are a function of location as well as time. Thus different points in HAZ undergo different changes at the same time.

In such a situation the only alternative available is to undergo simulated studies. These simulated studies can be carried out on a larger specimen for any point in HAZ of the welded member by simulating the weld thermal cycle of that point on the specimen. Both experimental and theoretical methods could be applied for these simulation.

Many research workers like Savage and others [2] did

primary work on weld thermal simulation technique, as reported in the literature review, but the modern technique is developed by Clifton et al.[3] in the form of a closed loop weld thermal simulator. The system consists of a thermocouple embeded in the specimen, the output of which is continuously compared with the reference voltage generated by function generator. The error signal is fed to control the power supply to the heating system of the specimen.

Modern simulators, with programming and feed back control system, are capable of generating and controlling the weld thermal cycle in the fine limits at the expense of higher cost with extremely complicated systems. Complications, safety requirements and higher cost has confined its use in the sophisticated laboratories. In the light of these points, it is extremely necessary to evolve a simple system of simulation with comparable end results. It will be preferable to use traditional same sources of heat as is available in the welding shops itself such as gas flame or electric arc.

In any welding process, the thermal cycle mainly consists of:

i. Heating portion

ii. Peak temperature and soaking time

iii. Cooling curve.

The rate of heating has got almost no or little effect on the metallic properties in the final conditions, thus it is not considered in thermal simulation. Heating rates in welding

are very fast, thus complete repetition of this portion on a simulated specimen leads to the requirement of a huge amount of power and extensive control system. This portion is responsible for the major cost of the simulation set up.

Peak temperature, above the critical temperature, extremely effect the microstructure and mechanical properties of metals. In this regard, only decision required is whether the peak temperature is above the critical temperature or below it. Soaking time above critical temperature will effect the grain size but due to faster heating and cooling cycle, the actual soaking time in welding is very small.

Adrichan and Kas [4] reported that cooling rate, particularly in the temperature zone of 800°C to 500°C, has maximum effect on the properties of simulated specimens, because different phases of steel at room temperature depends upon the cooling rate in a temperature zone of 500°C to 800°C. This intern can be evaluated by time taken to cool from 800°C to 500°C.

In view of foregoing objections of closed loop simulation technique, it was thought desirable to develop a simple weld thermal simulator using welding gas flame in which only two parameters namely peak temperature and cooling rate in the zone of 800°C to 500°C were controlled. A computer programme was also developed to simulate thermal and metallurgical changes in low alloy steel as a result of welding process. Computer aid results were then compared with experimental results.

CHAPTER - 2

LITERATURE REVIEW

2.1 GENERAL REMARKS

Pioneering work in the direction of weld thermal simulation was done by Savage et al.[1]. They passed large a.c. current through the specimen to get rapid heating rates. They made attempts to duplicate the weld thermal cycle by programming heating current as a function of time. However, with trials and error method by taking thirty to forty trials, it was possible to obtain a correspondence within $\pm$ 50°C of desired thermal cycle.

Later on Clifton et al.[3] developed a closed loop thermal simulator. In this simulator, the output of the thermocouple attached to the specimen is continuously compared with the reference voltage generated by the function generator and the error signal is used to control the power supplied for heating the specimen. This system is capable of controlling the specimen temperature within $\pm$ 20°C of the desired thermal cycle in a reproducible fashion.

In this chapter, the development of thermal cycle and various simulation techniques used to simulate it, is discussed. Design and construction of closed loop thermal simulator along with problems and limitations connected with it is given. A Δt approach on which the open loop thermal simulator is developed is also given. Apart from it, different tests which can be carried out during and after simulation is discussed.

2.2 THERMAL CYCLES

2.2.1 Actual Welding Conditions

Heat inputs to base metal in fusion welding is usually through flame, electric arc and energy beam. Heat inputs from these sources produces very high temperature and the plate thus creates a molten weld pool, by melting the base metal and the filler metal. Heat from the molten weld pool and the heat source is transmitted to comparatively cooler portions of the base metal by all the three modes of heat transfer i.e.,conduction, convection and radiation. As a result of this,different points on the base metal will have different temperatures. Moreover, heat source in welding is not stationary one but moves at a constant speed, so temperature at any point on base metal is a function of time.

In welding, weld metal and base metal encounters a temperature above the melting point and solidifies under an equivalent of chill casting conditions. Thus the base metal encounter a very high heating and cooling cycle. Moreover as stated, all points in HAZ of base metal with different distances from the fusion boundary, will experience a different thermal cycle, consisting of rapid heating and cooling as shown in Fig.1. The peak temperature distribution and rates of heating and cooling can be achieved, which vary widely and depend upon welding process variables such as heat input, plate thickness and degree of preheat [3].

2.2.2 Theoretical and Experimental Models

Two approaches are available to find out the thermal cycle experienced by any point in HAZ. One is the theoretical approach and another is the experimental approach.

In theoretical approach, heat transfer in plates is tackled either as a two-dimensional or a three-dimensional case. For two dimensional case, considering heat source as a line heat source, with length equal to the thickness of the plate and assuming that the heat from the source is transmitted in X and Y directions only [5]. The resulting equation, applying boundary conditions, for uni-axial heat transfer is

$$T - T_o = \frac{q'}{2\pi K} e^{-v\xi/2\alpha} K_o\left(\frac{VR}{2\alpha}\right) \quad \ldots\ldots (2.1)$$

And the theoretical cooling rates [6] for any point (X,Y,Z) relative to the source as origin, for two-dimensional case is given by the following equation

$$\frac{dT}{dt} = -\frac{V^2 T}{2\alpha}\left[\frac{\frac{X}{R} K_1\left(\frac{VR}{2\alpha}\right)}{K_o\left(\frac{VR}{2\alpha}\right)}\right] \quad \ldots\ldots (2.2)$$

Similarly for three-dimensional case, while considering Z axis in the direction of thickness of plate and applying boundary conditions, the resulting equation for heat transfer becomes [5]

$$T - T_o = \frac{q}{4\pi KR} e^{-v/2\alpha(R+\xi)} \quad \ldots\ldots (2.3)$$

And theoretical cooling rates is given by the following equation [6]

$$\frac{dT}{dt} = -\frac{VT}{R}\left[\frac{X}{R} - \frac{VR}{2}\left(1 - \frac{X}{R}\right)\right] \quad \ldots\ldots (2.4)$$

Using above equations, the thermal cycles of various points in HAZ at right angle to a weld with a heat input $q/v = 4 \times 10^4$ joules/cm in 1.25 mm thick steel plate, were obtained as shown in Fig. 1.

Clifton and George [3] experimentally found thermal cycles for various points having different distances from the fusion boundary in case of a butt weld, carried out on 3/4 inch (19 mm) thick plate, with no preheat, at a heat input of 71 KJ/in (2.8 KJ/mm) as shown in Fig. 2.

2.3 SIMULATION TECHNIQUES

2.3.1 Various Simulation Techniques

Simulation techniques of a weld thermal cycle are either experimental or theoretical. Experimental simulation is carried out by the use of open loop and closed loop simulation systems. Closed loop simulation system involves a feed-back control of temperature and deformation courses in the specimen. Principle of operation of a closed loop simulator as explained in Fig. 3, is that a metallic specimen held in water cooled copper jaws is subjected to a given thermal cycle, with the help of a power generator. The output of the thermocouple attached to the specimen is continuously compared with the reference voltage obtained from the function generator. The error signal is fed back to the power controller which accordingly adjust the power of the generator [7].

Open loop simulation system do not have feed-back control of temperature and deformation courses in the specimen. Some research workers [4] has suggested the development of open loop simulation technique on Δt approach, which make this technique preferable for many considerations.

Theoretical simulation involves the development of a computer programme to simulate thermal and metallurgical changes in the base metal as a result of a welding process.

2.3.2 Closed Loop Simulation System

The closed loop simulator may conveniently be divided into three parts [7]:

i. Function Generator

ii. Heating and Heating Control System

iii. Specimen Holding and Cooling Device

Function Generator

In the closed loop simulator, function generator has to play a very important role. It has to produce a reference voltage as close as possible to the existing thermal cycle and yet flexible enough to accommodate the variation in different thermal cycles.

In early experiments, a predetermined thermal cycle was reproduced by using cam operated potentiometer to generate a voltage versus time reference cycle. Later on scientists suggested more promising methods to generate a reference voltage for a given thermal cycle.

Lower et al.[7] suggested a precision multi-turn potentiometer which produces the variable reference voltage representing the thermal cycle. The slides of this potentiometer is driven by a small d.c. motor, and the speed of the motor can be changed at selected points on the thermal cycle, thereby altering the slope dv/dt. A ten-point setting potentiometer is used to determine the voltage and hence the temperature at which the motor speed is changed, and this setting is preselected. At the appropriate moment a relay switches the preselected slider voltage into the input of a differential amplifier where the voltage output is compared with that of the main reference voltage potentiometer. When coincidence is reached i.e., at a selected temperature, the programme is advanced by one step, thus selecting the next phase of the function. The complete function thus consists of a series of straight lines which approximate closely to the required thermal cycle.

Clifton and George [3] used a single turn potentiometer, having number of taps equally spaced over a resistance range, is driven at a constant speed by driving motor and gear arrangement. A variable resistor is connected in series with the potentiometer and stabilised d.c. potential is connected across the terminal. By adjusting the tap to which the positive voltage connections to the net work is made and by adjusting the value of series resistor, the shape of the output function is varied. Further, by modifying the total resistance value at each tap position by suitable parallel resistors consisting of a bank of

multi-turn potentiometers, the voltage-time function is modified to produce shape function equivalent to that of the required function.

Heating and Heating Control System

Electric power is usually used to simulate the complete weld thermal cycle under full control for a wide range of specimen sizes.

Two mostly used methods of heating the specimens by electric power are:

i. Resistance Heating

ii. Induction Heating

Resistance Heating

In resistance heating a.c. power of low impedance is given to the specimen so that the specimen is heated by its own electrical resistance. The provision of the necessary power at low impedance is a considerable problem but a welding transformer as an impedance converter may be used as a ready source of the necessary power.

A further problem in resistance heating is that of pick up of heating current [6] by the thermocouple. Savage has described how this can be overcome by the use of a synchronous chopper which cuts off the heating current briefly during each half cycle and samples the thermocouple output during this period.

Induction Heating

In this heating system, high frequency induction heating is employed. Most induction heating systems use cylinderical testing coils. Square coils may also be used for square cross-section specimens.

In H.F. Induction heating the problem of classical skin effect [7] is there. Due to skin effect the temperature of the inside of the specimen lags behind that of surface during heating and thus variation in austenite grain size, across the specimen is evident. The problem was substantially eleminated by introducing a small holding period at peak temperature, allowing the centre to reach the surface temperature prior to cooling. As a consequence, the uniformity in grain size across the section was markedly improved.

Comparison

Induction heating system needs a more costly supply and that is why it is recommended for smaller specimens. The problem of skin effect is associated with it which can be overcome by providing small holding period at peak temperature.

Resistance heating system is comparatively cheaper and may be used for heating large size specimens. It has got the problem of heating current pickup which can be overcome by using synchronous chopper as suggested by Savage [2].

Heating Control System

The function of the heating control system is to compare the output of the thermocouple attached to the specimen with the

reference voltage from the function generator, and to use the resulting error signal to regulate the primary current in the power transformer, and thus helps in achieving the required cycle on the specimen.

The theory of control system design is well developed, but the requirement for very accurate temperature control, for a wide range of specimen sizes and heating rates, makes the control circuit design usually critical.

Specimen Holding and Cooling Device

The grips in which the specimen is held have two main functions [8]:

i. To conduct heat from the specimen.

ii. To provide a mechanical support and transmit test loads to the specimens.

In case of resistance heating these also conduct heating current to the specimen.

Clifton and George [3] used specimen grips which consists of four copper blocks, through which water is circulated. Each end of the specimen is gripped between two blocks by means of four bolts.

One of the specimen grip is free to move to accommodate expansion and contraction, as the specimen heats up and cooled down. The free specimen grip is mounted on a ball-bearing slide, so that it can take care of expansion and contraction of the specimen.

Cooling in copper grips is achieved by circulating water through them, ensuring that the maximum cooling rate (in the absence of any heating) is greater than that needed for simulation of required thermal cycle. So that the cooling rate can be controlled by maintaining a small variable heat input to the specimen, during the cooling part of the cycle.

2.3.3 Problems Connected with Closed Loop Simulation System

Closed loop simulators developed by different scientists till today has got numbers of short-comings as given below [7,8]:

i. The whole system becomes expensive due to its costly elements, function generator one of the essential element, involves multi-turn potentiometer, ten-point potentiometer, d.c. motor etc. The heating system consumes large a.c. power in resistance heating and high frequency current in induction heating to get fast heating rate as required in thermal cycle. These all factors make this simulator a costly one [7,8].

ii. The system is more time consuming as the complete thermal cycle is to be simulated with feed-back.

iii. The system is complicated due to its heating and feed-back system. To get reference voltage, settings in function generator is to be done, and in heating system due to rapid heating, large a.c. power at low impedance or high frequency current is a problem [8].

iv. As the heating system involves large a.c. current or high frequency current, it becomes less safe to use it [7,8].

v. The heating system used has got some technical problems, as in resistance heating the pick up of heating current by thermocouple is obvious which give wrong readings of temperature measurements [8]. Induction heating system has got the problem of critical skin effect, by which the temperature at the centre of the specimen lags behind that of at surface [7].

vi. Inspite of all this preciseness and control on temperature these simulators are unable to produce the real welding condition prevailing in a HAZ.

2.3.4 Δt Approach

In steel, above the critical temperature, different phases of it converts into austenite and on cooling the austenite converts back into pearlite, bainite or in austenite depending upon the cooling rate. For cooling rates faster than critical cooling rate the austenite converts into martensite. It is observed by scientists [4] that different phases of steel at room temperature depends upon the cooling rate in a temperature zone of 500°C to 800°C. This intern can be evaluated by time Δt taken to cool from 800°C to 500°C. Figure 4 defines the important time interval Δt required for cooling from 800°C to 500°C, on temperature-time curves.

In principle, the length of Δt can be calculated by making use of the known theories concerning heat-distribution during welding.

From the Rosenthal equations (2.1) and (2.3), Δt for the weld centre may be calculated and is given by [4]

$$\Delta t = \frac{1}{2\pi K}\left(\frac{q}{v}\right)\left(\frac{1}{500 - T_o} - \frac{1}{800 - T_o}\right) \quad \ldots\ldots (2.5)$$

for welding thick plates (three-dimensional cooling) and

$$\Delta t = \frac{1}{4\pi K \rho C}\left(\frac{q}{vg}\right)^2\left[\left(\frac{1}{500 - T_o}\right)^2 - \left(\frac{1}{800 - T_o}\right)^2\right] \quad \ldots\ldots (2.6)$$

for welding thin plates (two-dimensional cooling). The heat loss to ambient atmosphere not being taken into consideration.

The choice of the formula is governed by the plate thickness, the welding data and the properties of the base material. The decision can be made by calculating transion plate thickness d'. Cooling will be three-dimensional for plate thickness exceeding d' and otherwise it will be two-dimensional. By equating equations (2.5) and (2.6), the transion plate thickness can be found as [4]

$$d' = \sqrt{\frac{q}{2\rho Cv\left(\frac{1}{500 - T_o} + \frac{1}{800 - T_o}\right)}} \quad \ldots\ldots (2.7)$$

2.4 TESTS CARRIED OUT

These can be categorised into two groups:

i. Tests carried out during the simulation cycle.

ii. Tests carried out after the simulation cycle.

2.4.1 Tests During Simulation

Tests during simulation are mainly [9]:

i. Dilatometry test

ii. Hot ductility test.

Dilatometry Test

Dilatometry test is carried out to detect metallurgical phase transformations at high heating or cooling rates in metals, characteristics of welding and heat-treatment processes [9].

A dilatometer consists of a pair of quartz knife edges, coupled to a solid hinge liver mechanism and a high resolution rectilinear potentiometer. The quartz knife edges contact the specimen across the diameter [10], and any expansion or contraction in the specimen is transmitted to the potentiometer via the solid hinge. This in turn produces a signal on the chart recorder directly proportional to the dilation and since the dilation recording is simultaneous with the recording of temperature, it is claimed that phase transformations can be readily detected.

Hot Ductility Test

The simulator has been used to investigate the high temperature ductility of several high yield strength, quenched and tempered low alloy steels.

In such investigations the principal approach has been the measurement of 'on heating' and 'on cooling' tensile characteristics, mainly ductility, with the object of relating differences in 'on heating' and 'on cooling' behaviour to the

performance of the steels in weldability tests giving an indication of susceptibility of HAZ hot cracking [11].

2.4.2 Tests After Simulation

Tests carried out after simulation are numerous, the most common are impact test and fracture mechanics test.

Impact Test

The most common test after simulation is Charpy v-notch test [11]. In this test, simulated specimen are notched using schnadt cutter, which has got excelemt reproducibility of notch radius. The notch is located in such a way so that it removes the thermocouple bead. It is known that steels like most other BCC metals and alloys absorb more energy when they fracture in a ductile fashion rather than in a brittle fashion, so the impact test is often used to assess the temperature of the transition from the ductile to brittle state which occurs as the temperature is lowered.

Fracture Mechanics Test

The subject of fracture mechanics deals with the study of fracture of materials. One of the most dangerous types of failure is failure by brittle fracture. For example, the brittle fracture of the hulls of 'Liberty Ships' during Second World War. Crack opening displacement (COD) test is commonly used to determine the sensitivity for brittle fracture [12]. The COD test can be performed as tensile or bending test. The specimens prepared has got a notch which consists of two parts, viz., a mechanical part and a fatigue part.

During the test, the opening of the notch can be determined on one or more levels by means of a clip gauge with strain gauges. The clip gauge consists of a pair of spring steel strips with small diamonds at the end. The clip gauge is placed into the notch, they press against the surfaces of the notch by means of the diamonds and they follow the surfaces when the notch is opened under load. When this (these) opening(s) has(have) been determined, the opening in the bottom of the notch at the moment of fracture can be calculated. The opening in the bottom of notch, at the moment the first crack starts gives an indication about the toughness of the material.

CHAPTER - 3

EXPERIMENTAL WORK

3.1 OBJECT

Comparing the open loop and closed loop simulation, it is evident that cost wise open loop simulator is better than closed loop, as its cost is extremely low. The effected accuracy may be very little in comparison with the reduction in cost. So it was decided to fabricate an open loop thermal simulator.

A thermal cycle involves heating rate, peak temperature, soaking time and cooling rate. In welding, the thermal cycle of a point in HAZ near weld pool involves fast heating rate, peak temperature above critical value, very small soaking time and moderate cooling rate. Out of these factors only peak temperature and cooling rate has got main effect on the structure and properties of the simulated specimen. Moreover as discussed, different phases of steel at room temperature depends upon cooling rates in a temperature zone of 500°C to 800°C [4]. These cooling rates can be evaluated by time taken to cool from 800°C to 500°C. It is also known that austenite grain size depends upon austenitizing temperature, time to austenise and the cooling rate in the critical zone. So the simulator was designed to control the cooling time in critical zone, along with manual control of peak temperature.

3.2 EXPERIMENTAL SET UP

General arrangement of various components of this set up are shown in Fig. 5a,b. It consists of a cylindrical specimen of

mild steel with a 0.14 per cent carbon contents. Different specimens were prepared to 1 cm diameter and 24 cm long. With these dimensions, it is possible to carry out hardness structure and COD testing etc. and at the same time chances of temperature variations along the cross-section are very little.

The specimen is heated from one end where as the other end supports it during the complete cycle. A special rectangular frame along with the stand, was fabricated to support these specimen. One end of specimen rests in a hole in the block of a frame. The heating side of the specimen is insulated from frame by placing the heat resistant plate between specimen and the frame.

Since heating rate is not important in this type of simulation, any mode of heating which is capable of giving desired peak temperature can be used. As such commonly used mode of welding i.e., oxy-acetylene gas flame was used. The heating was done from one end only. By manual control of distances, peak temperature can be controlled. As the required peak temperature and soaking time was reached, the heating isstopped.

Rate of cooling,after the heating,was controlled by passing cold water around the specimen through a water jacket. Internal diameter of water jacket is equal to the diameter of the specimen plus allowance so that this jacket can be easily slipped over the specimen. Outside diameter of the jacket is 8.75 cm and thickness 3.5 cm. The distance of water jacket from the thermocouple can be adjusted with a pointer and scale arrangement. A thermometer was attached to measure the inlet temperature.

Amount of water was controlled through a cock, and measurement of discharge was done through a graduated jar and stop watch.

Temperature measurement was done by a chromel-alum thermocouple having a range from 0°C to 1350°C. A hole of 2 mm x 4 mm was made in each specimen to fix the thermocouple. Thermocouple wires are protected from direct gas flame by heat resistant beads and sleeves. These thermocouple wires are connected to recorder having arrangement for signal amplification and chart plotter. A chromel-alum calibrated temperature indicator was also attached in parallel to have a counter check.

3.3 EXPERIMENTAL PROCEDURE

In order to check the repeatability, number of independent observations for peak temperature and cooling rate in the critical temperature range was recorded. In the first, the specimen along with jacket was placed in position. Discharge setting was carried out by setting the position of the cock and checking the same at the other end with the help of a graduated cylinder and a stop watch. After setting the discharge, the flow through jacket is stopped by a valve which is only used to open or close the flow through the jacket.

Thermal cycle started with the heating of a specimen. Heating was completely a manual operation in which a desired peak temperature of 900°C has to be attained. After few initial trials the welder was able to obtain it. Soaking time at peak temperature, indicates how far a welder was able to maintain the peak temperature for a longer time.

After completing the heating cycle, the heating is stopped and water circulation is started. The rate of cooling was dependent upon the distance of sink and point under consideration, when the discharge and inlet temperature are kept constant. Time measurement from 800°C to 500°C was recorded with stop watch and verified with chart from the recorder. One such chart record is shown in Fig. 6a,b. For establishing the reproducibility of the experimental system, ten trials were made and values of peak temperature T_a, cooling time Δt from 800°C to 500°C, heating time t_a and soaking time were recorded as given in Table 1.

After ascertaining the reproducibility of the experimental system, some of the specimens were exposed to different thermal cycles by changing the cooling time from 800°C to 500°C as shown in Tables 2 and 3. Value of peak temperature was tried to maintain constant at 900°C.

These specimens were prepared for hardness testing. Specimens were cut at the location where thermocouple was embeded. Thin outer layer was removed by the grinder so as to eliminate the possible effect of atmospheric contamination or carbon diffusion during heating.

As planned, hardness measurements were made both in the radial and transverse directions, so that any variations could be recorded. Hardness measurements were carried out on a Rockwell hardness testing machine using hardened steel ball on scale 'B', at equal intervals. The observations so recorded are shown in Tables 2 and 3, and curves were drawn accordingly as

shown in Figs. 7 and 8 for radial and transverse direction respectively.

The microstructure of the samples, subjected to simulated welding conditions, were also studied. The specimens were cut at the regions, where the temperatures were taken and then polished with usual mechanical abrasion techniques. After that the samples were etched with 2 per cent Nital (2 per cent HNO_3 and 98 per cent alcohol) for 45 seconds. The metallographic studies were conducted on a large incident light camera as Neophot 2. The microstructures were examined at different magnifications throughout the specimen.

CHAPTER - 4

THERMO-METALLURGICAL COMPUTER AIDED SIMULATION

4.1 INTRODUCTION

Computer aided simulation can be suitable alternative approach in comparison with the hazardous and time-consuming experimental approach. It can be more useful than experimental simulation as it will be extremely cheap to simulate various factors connected with it.

In computer programme, it is easy to incorporate changes as and when required. Study of possible alternatives can be implemented. Optimisation studies of welding parameters can be easily carried out with its help. It provides very quick results to designer or a research scholar. With this in mind, an attempt has been made to develop a computer programme, which can simulate thermal and metallurgical changes in low alloy steel as a result of welding process.

4.2 DEVELOPMENT OF COMPUTER PROGRAMME

Welding process may be simulated as a heat source moving over the metallic members to be joined together. The heat source transmits the heat to the metallic plates, which is further conducted away to the comparatively cooler sections of it. It results in solidification and thus joining of the two plates together. This process produces a thermal cycle consisting of heating and cooling portions. Temperature at any point in the heat affected zone of the plate will be a function of time. Range

of temperature involved will be a temperature higher than the melting point of the metal considered to a temperature as low as room temperature.

This thermal cycle will produce changes in grain size, phase transformation and changes of mechanical properties depending upon the chemical composition of the steel or metal.

Accordingly, the computer programme has been given the modular construction so that different sets of information can be added or deleted, depending upon any advancement concerned. Programme mainly consist of:

i. Input information
ii. Calculation of critical cooling time
iii. Calculation of austenite grain size
iv. Interpolation of CCT curve
v. Factors affecting the shift of CCT curve
vi. Actual shifting of CCT curve
vii. Phase change
viii. Calculation of hardness.

4.2.1 Input Information

Input information to the computer programme consist of welding conditions, geometry and chemical composition of the base metal. The value chosen for these parameters are given in Table 4.

4.2.2 Calculation of Critical Cooling Time

Quantitatively, the heat flow and temperature distribution

to be found are governed by welding parameters, the joint geometry, the heat flow distribution of the arc, the heat exchange between the work-piece and the environment and by the thermal properties of the base material [4]. In view of the high degree of complications involved in a strict mathematical treatment, it is essential to develop appropriate models stressing all primary features and discarding secondary peculiarities. Rosenthal's model for temperature distribution [5] has been made accordingly and is used in our study.

Depending upon the welding conditions, one of the two models can be chosen for temperature distribution [5].

i. Three-dimensional (3D) heat flow model in which a semi-infinite body with heat flow in three directions from a moving point source and zero heat loss through the top surface is considered.

ii. Two-dimensional (2D) heat flow model is based on the heat flow in two directions from a moving line source when plate is considered to be a thin plate. In this case temperature in thickness direction is assumed to be constant.

There are models in between the two, but in HAZ one of the two models can be safely considered.

Peak temperature and cooling time corresponding to critical zone is important from the point of view of metallurgical and mechanical properties. This critical zone for steel can approximately be taken from 800°C to 500°C [4].

Adrichen and Kas [4] performed certain experimental and analytical work and concluded that the cooling time from 800°C to 500°C in the heat affected zone and the weld centre differ very slightly, as such it can be approximately taken to be equal for simplification purposes.

In these conditions, Rosenthal's equations (2.1) and (2.3) given in literature review are simplified considerably and thus it is possible to express critical cooling time (Δt) interms of certain variables as shown below [4]

$$\Delta t = \frac{1}{2\pi K}\frac{Q}{V}\left[\frac{1}{500 - T_o} - \frac{1}{800 - T_o}\right] \quad \ldots\ (4.1)$$

(for 3D cooling)

$$\Delta t = \frac{1}{4\pi K \rho C}\left(\frac{Q}{Vg}\right)^2\left[\left(\frac{1}{500 - T_o}\right)^2 - \left(\frac{1}{800 - T_o}\right)^2\right] \quad \ldots\ (4.2)$$

(for 2D cooling).

By equating the two cooling time equations, the transion plate thickness d' can be found as [4]

$$d' = \sqrt{\frac{Q}{2\rho Cv}\left(\frac{1}{500 - T_o} + \frac{1}{800 - T_o}\right)} \quad \ldots\ (4.3)$$

Depending upon various welding and geometrical parameters, first a decision has to be made for the suitability of 2D or 3D model. In this regard, the transion plate thickness (d') is calculated and compared with the plate thickness (d). If $d > d'$ then it is considered a three-dimensional case, otherwise two-

dimensional case and equations (4.1) and (4.2) are used accordingly for the calculation of critical cooling time Δt.

4.2.3 Calculation of Austenite Grain Size

If the temperature at a point in HAZ has crossed critical temperature, the resultant structure and properties will depend upon the cooling rate in the critical zone, the peak temperature and chemical composition of steel. For calculation of austenite grain size, curves from reference [13] of austenite grain size as a function of cooling time from 800°C to 500°C at different peak temperatures were considered. Equation drawn from these curves is explained in Appendix-I. Effect of soaking time being small is neglected. The resulting equation is fed to computer programme, for the calculation of austenite grain size.

4.2.4 Interpolation of CCT Curve

It may be difficult to incorporate variety of CCT curves available for steels, so a generalised CCT curve obtained from reference [14] at page 718 regarding low alloy steels having different formation zones for marten-site, bainite and peralite, depending upon the cooling time in critical zone is considered. The curve has been simplified by replacing the curves with appropriate straight lines as shown in Fig. 9.

In the assumed CCT curve, log of cooling time in critical zone is represented on X-axis and temperature on Y-axis as in the case of most of the CCT curves available in the literature. Salient points in this curve includes the representation of

total formation of martensite, which is represented by a horizontal straight line of length A. This line is followed by another horizontal straight line from A to AX. In this zone a combination of martensite and bainite is formed. Further, a slanted straight line from AX to AZ with a positive slope is assumed. In this zone Bainite and ferrite/peralite is the most probable structure to be formed. After AZ the cooling rate is extremely slow, resulting in the formation of a structure almost available in the equilibrium conditions. The value of AX and AZ is represented interms of A and fed into the computer programme. These values are determined from the considered CCT curve and are as under AX = A + 1.10 and AZ = A + 1.50.

4.2.5 Factors affecting the Shift of CCT Curve

The shift position of CCT curve on abcissa is dependent on the chemical composition and austenite grain size. The main elements of chemical composition, which effects the shift of CCT curve, includes C, Mn, Si, Ni, Cr, and Mo. Knowing the percentage content of these elements, the hardenability multiplying factors, which indicates the shift of CCT curve due to chemical composition can be find out from Table 5, obtained from reference [14]. Effect of these elements and austenite grain size are included in the computer programme in the form of equations through hardenability multiplying factors as explained in Appendix-II.

4.2.6 Actual Shifting of CCT curve

The base diameter X_5 incorporate the total effect of

chemical composition and austenite grain size. Actual shifting of CCT curve on X-axis is calculated by finding the time of cooling through critical zone at a base diameter from the heat source [15]. In this regard, semi-infinite body with a heat source in the centre was considered. Based on these assumptions Δt is given as under

$$\Delta t = [(\frac{X_6}{1.2})^2(\frac{DI}{DE.TC})].$$

Now the revised value of 'A' will include the initial value plus the log Δt.

4.2.7 Phase Change

Once the actual location of the CCT curve based on chemical composition and austenite grain size is known, it will be easy to predict an anticipated phase formation for any cooling rate. Depending upon the actual cooling time from 800°C to 500°C in HAZ, calculated by equations (4.1) and (4.2), the final phase will be a certain proportion of martensite, bainite, peralite/ ferrite etc. Their ratio can be calculated from the CCT curve as explained in Appendix-III and the information is fed to computer programme.

4.2.8 Calculation of Hardness

The hardness at any point in steel is determined by the type of phase and the carbon content. Linear relations are interpolated from the experimental information,obtained from reference [14], as explained in Appendix-IV. Hardness of the combination of two phases will be in proportion to its constituents.

CHAPTER - 5

DISCUSSION ON THEORETICAL AND EXPERIMENTAL RESULTS

5.1 REPRODUCIBILITY OF EXPERIMENTAL DATA

For the purpose of establishing reproducibility of the experimental data, a number of independent observations for peak temperature T_a, heating time t_a, soaking time and cooling time from 800°C to 500°C were recorded as shown in Table 1. Total ten specimens were taken and standard deviation for peak temperature T_a and cooling time from 800°C to 500°C were calculated. Standard deviation for peak temperature came out as 4.683 and for $\Delta t_{800^\circ C - 500^\circ C}$ as 1.523.

5.2 HARDNESS IN HAZ

Hardness measurements in radial and transverse directions were carried out for seven specimens at different cooling rates. The observations as Rockwell hardness on 'B' scale for radial and transverse directions is given in Tables 2 and 3 respectively. Graphs were also plotted against these observations as shown in Figs. 7 and 8. Curves in Fig. 7 are almost straight lines which indicate that hardness remains almost constant in radial direction. In Fig. 8, the curves make an abrupt downward trends after 3 mm of distance from surface in transverse direction and then onwards remain almost a straight line. This behaviour of the curves suggests that the HAZ of the samples is upto 3 mm of distance from the surface in transverse direction and after that there is no or little effect on hardness.

5.3 COMPARISON BETWEEN THEORETICAL AND EXPERIMENTAL RESULTS

Hardness results obtained by theoretical as well as experimental simulation system were compared.

Cooling time from 800°C to 500°C in seconds was taken on X-axis and rockwell hardness on 'B' scale on Y-axis. Experimental and theoretical hardness curves were then plotted as shown in Fig. 10, from experimental hardness results given in Table 2 and theoretical hardness results given in Table 6.

The trend for both the curves is almost same i.e., with decrease in cooling time, hardness increases.

The theoretical curve is below the experimental curve and the gap between them decreases and becomes zero at value of $\Delta t_{800^{\circ}C - 500^{\circ}C}$ equal to 54 seconds. This indicates that theoretically determined hardness values are comparatively less than the experimentally determined hardness values. This can be explained by the following reasons:

i. CCT curve for simplification purposes is taken to be a straight line instead of a curve.

ii. There may be some effect of soaking time on final structure and hardness, which have been neglected in this study.

CHAPTER - 6

CONCLUSIONS

In view of the foregoing discussions of the results, the following conclusions can be drawn:

i. It is possible to use a relatively inexpensive simple weld thermal simulator without a closed loop system.

ii. A chosen temperature cycle can be reproduced with small errors. The standard deviation for peak temperature came out as 4.683 and for $\Delta t_{800^{\circ}C - 500^{\circ}C}$ as 1.523 for open loop flame heated weld thermal simulator.

iii. In open loop flame heated weld thermal simulator a minimum of 25 seconds as a cooling time from 800°C to 500°C is possible.

iv. Uniformity of hardness variation is possible in whole radial direction and upto HAZ in transverse direction for the considered specimen.

v. It is possible to simulate the anticipated hardness of a specimen with the help of a computer.

vi. Theoretical results for hardness, obtained by computer aided simulation, resembles with the experimentally obtained results.

vii. For simulated weld specimen, the variation between cooling rate and hardness is linear. Moreover, as the cooling time decreases, the hardness increases.

CHAPTER - 7

SUGGESTIONS FOR FUTURE WORK

i. Computer aided simulation should be improved by incorporating more accurate cooling CCT curve.

ii. Further experimentation is suggested with other parameters of simulation so that data can be generated for comparison.

iii. For comparison purposes, other tests during and after simulation should be considered for theoretical as well as experimental simulation system.

REFERENCES

[1] Nils Stenbacka,
'A Simple Weld Thermal Simulation Technique with Induction Heating',
Scandinavia Journal of Metallurgy, 6(1977),pp 271-281.

[2] Savage, W.F.,
'Evolution of the Gleeble',
A Research Application Seminar, London,27th Apr 1972.

[3] Clifton, T.E. and George, M.J.,
'Design and Construction of a Weld Heat Affected Zone Simulator',
Metal Construction and British Welding Journal,Sep '69.

[4] Th. J. Van Adrichen and J. Kas,
'Calculation,Measurement and Simulation of Weld Thermal Cycles',
Holectechnick 1(1971)1.

[5] Rosenthal, D.,
'Mathematical Theory of Heat Distribution During Welding and Cutting',
Welding Research Suppliment 220-234 May 1941.

[6] Lancaster, J.F.,
'The Metallurgy of Welding Brazing and Soldering',
George Allen and Unwin Ltd.,London.

[7] Lowes, J.M., Richardson, K.D., and Hadrill, D.M.,
'A Thermal Simulator Employing Induction Heating',
A research Application Seminar,London,27th Apr 1972.

[8] Widgery, D.J.,
'The Design and Use of Resistance - Heated Weld Thermal Simulators',
A Research Application Seminar,London, 27th Apr 1972.

[9] Keane, D.M., Bower, E.N., and Hammond, J.,
'Tests During Simulation',
A Research Application Seminar,London, 27th Apr 1972.

[10] Howden, D.G.,
'Isothermal Transformation Characteristic of a Low Alloy Steel Using A Weld Thermal Cycle Simulator',
Canadian Metallurgical Quarterly, Vol.6, No.3.

[11] Kilpatrick, I.M., Allan, R.C., and Main, R.,
'The Application of Thermal Simulation Techniques to the Assessment of the Mechanical and Metallurgical Properties of the HAZ in High Yield Steels',
A Research Application Seminar, London, 27th Apr 1972.

[12] Verburg, S.J.,
'The COD Test',
Machine Building Industry, Vol.15, No.1, Jan 1977.

[13] Berkhout, C.F.,
'A Comparison of the Microstructures in the Simulated and Weld HAZ',
A Research Application Seminar, London, 27th Apr 1972.

[14] Robert E. Reed - Hill,
'Physical Metallurgy Principles',
D.V.N. Company, New York.

[15] Kreith,
'Principle of Heat Transfer'.

APPENDIX-I

As shown in Fig. 11, experimental data on austenite grain size versus cooling time in the critical zone for a particular peak temperature can be nicely fitted into a straight line. Another salient feature of these curves is that as the peak temperature increases, grain size reduces, more or less uniformly.

Keeping this in mind, it was decided to introduce a straight line equation for grain size, regarding the variation of both cooling time and peak temperature.

General equation of a straight line is $Y = MX + C$, where M is the slope of the straight line and C is the ordinate corresponding to zero axis.

In our considered graph, the slope of the lines is negative, so our equation become $Y = C - MX$. The values of C and M are found as follows:

Values of M

Slopes M_1, M_2 and M_3 for straight lines 1,2 and 3 can be calculated as shown below:

$$M_1 = \frac{9 - 8}{100} = 0.01 \qquad M_2 = \frac{5.5 - 3.5}{100} = 0.02$$

$$M_3 = \frac{2.5 - 1}{100} = 0.015$$

$$\text{So average slope } M = \frac{M_1 + M_2 + M_3}{3} = \frac{0.045}{3} = 0.015$$

Value of C:

The value of grain size at 1000°C peak temperature, corresponding to Δt = 100 seconds is 8, whereas for 1350°C peak temperature it is 1, as indicated in the figure. Thus if straight line relation is assumed in grain size versus peak temperature, then at 1400°C peak temperature the grain size will be zero at cooling time Δt = 100seconds. So

$$C = \left(\frac{1400 - PT}{400}\right)8$$

Thus the complete equation become as such

$$G.S = \left(\frac{1400 - PT}{400}\right)8 - 0.015\ \Delta t.$$

APPENDIX-II

Equations of hardenability multiplying factors, for various alloying elements in steel, has been derived from the experimental data given in Table 5 of reference [14], by plotting it as shown in Figs. 12 and 13. These figures explain the derivation of the said equations. Equations were later on used in computer programme.

APPENDIX-III

Ratio of various phases is evaluated from the assumed CCT curve as shown in Fig. 9.

i. If actual cooling time AL is less than the critical cooling time A, then only martensite will form.

ii. If AL is greater than A but less than AX, a combination of bainite and martensite may form. The ratio of martensite formed is evaluated by the 'lever Rule', assuming complete formation of bainite at AX and complete formation of martensite at A.

iii. If AL is greater than AX but less than AZ, then a combination of bainite and peralite/ferrite may form. The ratio of peralite and bainite is evaluated by the lever rule, considering complete formation of bainite at AX and complete formation of peralite/ ferrite at AZ.

iv. If AL is greater than AZ then only formation of peralite/ferrite is assumed.

APPENDIX-IV

Figure 14 from reference [14] at page 729, indicates the relation of percentage of carbon content with rockwell C-hardness of martensite. A linear relation could be assumed without much of error as shown in the figure. The relation derived from the curve could be assumed as follows:

$$MH = 25 + 35\ CC$$

This relation is obtained while finding the equation of a slanting straight line of slope $M = \frac{60 - 25}{1} = 35$ and $C = 25$.

Similarly, hardness equations for banite and peralite can be find out from reference [14] and are given as under:

$$BH = 5 + 35\ CC$$

and

$$HB = 40 + 20\ CC$$ respectively.

TABLE 1

Reproducibility of Experimental Data

Specimen No.	T_a	t_a	Δt	Soaking time	$(T_a-\bar{T}_a)^2$	$(\Delta t-\bar{\Delta t})^2$
1.	895.6°C	1'-18"	48"	1'-28"	11.628	0.01
2.	908.8°C	1'-16"	50"	1'-20"	77.26	3.61
3.	900°C	1'-17"	50"	1'-21"	29.05	3.61
4.	902.5°C	1'-17"	49"	1'-21"	8.35	0.81
5.	904.8°C	1'-18"	48"	1'-22"	0.34	0.01
6.	906.8°C	1'-18"	48"	1'-24"	0.37	0.01
7.	909.9°C	1'-18"	49"	1'-23"	0.01	0.81
8.	907.8°C	1'-18"	47"	1'-24"	5.80	1.21
9.	912°C	1'-19"	45"	1'-28"	43.69	9.61
10.	910°C	1'-19"	47"	1'-27"	21.25	1.21

$$\Sigma T_a = 9053.9^\circ C, \quad \bar{T}_a = \frac{\Sigma T_a}{n} = \frac{9053.9}{10} = 905.39^\circ C$$

$$\frac{\Sigma(T_a-\bar{T}_a)^2}{n-1} = \frac{197.38}{9} = 21.93, \quad S.D. = \sqrt{21.93} = 4.683$$

$$\Sigma\Delta t = 481, \quad \bar{\Delta t} = \frac{\Sigma\Delta t}{n} = \frac{481}{10} = 48.1"$$

$$\frac{\Sigma(\Delta t-\bar{\Delta t})^2}{n-1} = \frac{20.90}{9} = 2.322, \quad S.D. = \sqrt{2.322} = 1.523$$

TABLE 2

Rockwell hardness (B scale) values of various simulated specimen At different cooling rates from its centre in Radial direction

Specimen No.	Distance (mm) / Cooling Time from 800°C-500°C	Rockwell hardness (B scale) 0	1	2	3	4	Average rockwell hardness
1.	25"	82	82.5	80.5	81	81.5	81.5
2.	40"	64	65	64.5	65.5	65	64.8
3.	47.5"	60.5	60	60.5	60.5	61	60.5
4.	51"	57.5	58.5	59	58.5	60	58.3
5.	58"	55.5	55	55.5	55	54	55.0
6.	65"	51	50	49	50	51	50.2
7.	70"	48.5	49	48	47.5	47	48.0

TABLE 3

Rockwell hardness (B scale) values of Various simulated specimens at Different Cooling Rates in Axial Direction

Specimen No.	Cooling time from 800°C-500°C	Distance (mm) 1	3	5	7	9	11	13
		(Rockwell hardness (B scale)						
1.	25"	85	78	52.5	49	48	48	48
2.	40"	72	67.5	50	46	44.5	45.5	46
3.	47.5"	65	61	45	41	42	42.5	43
4.	51"	62.5	57.5	42	37.5	40	40	40.5
5.	58"	60	55	41	35	38	38.5	39
6.	65"	57	51	38	35	37.5	37.5	35.5
7.	70"	52.5	46	37	33	35	34.5	35

TABLE 4

Input Data of Computer Programme

FORMAT	F 8.4	F 8.2	F 8.4	I 4	F 8.4	F 8.4	F 8.4	F 8.4
VARIABLE	DI	MI	V	IT	DE	TC	TO	PT
VALUE	000.0200	03600.00	000.5000	0035	007.0000	000.2100	001.0000	905.3900

units of k

FORMAT	[6 (F 6.4), 10 X]					
VARIABLE	CC	CMN	M1	CMI	CR	CMO
VALUE	0.1400	1.0000	2.0000	1.0000	0.5000	0.5000

TABLE 5

Hardenability Multiplying Factors

Percent	Carbon Grain Size			Mn	Si	Ni	Cr	Mo
	6	7	8					
0.05	0.081	0.075	0.069	1.167	1.035	1.018	1.108	1.15
0.15	0.141	0.131	0.121	1.500	1.105	1.055	1.324	1.45
0.25	0.182	0.167	0.156	1.833	1.175	1.091	1.540	1.75
0.35	0.215	0.200	0.184	2.167	1.245	1.128	1.756	2.05
0.45	0.244	0.225	0.209	2.500	1.315	1.164	1.972	2.35
0.55	0.273	0.251	0.231	2.833	1.385	1.201	2.188	2.65
0.65	0.295	0.273	0.251	3.167	1.455	1.237	2.404	2.95
0.75	0.315	0.293	0.270	3.500	1.525	1.273	2.620	3.25
0.85	0.335	0.312	0.287	3.833	1.595	1.309	2.830	3.55
0.95	—	—	—	4.167	1.665	1.345	3.052	—
1.00	—	—	—	4.333	1.700	1.364	3.160	—

TABLE 6

Theoretically Obtained Rockwell Hardness Results for Different Cooling Rates

Sr. No.	Cooling time from 800°C to 500°C (seconds)	Rockwell hardness (B scale)
1.	23.195	78.3805
2.	25.573	74.716
3.	28.335	71.0271
4.	31.571	67.474
5.	35.395	63.960
6.	39.95	60.577
7.	45.463	57.385
8.	52.190	54.468
9.	60.528	51.925
10.	71.036	49.900

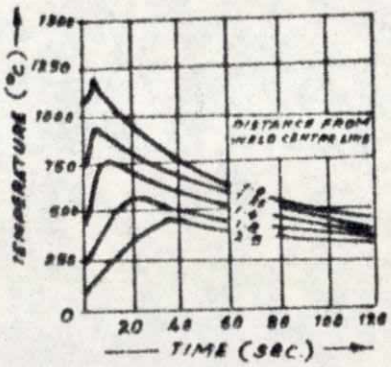

FIG. 1. THEORATICALLY DETERMINED THERMAL CYCLES AT VARIOUS POINTS ALONG A LINE AT RIGHT ANGLES TO A WELD MADE WITH A HEAT INPUT $\eta/v = 4 \times 10^4$ JOULES/CM IN 1·25 mm THICK STEEL PLATE. (5)

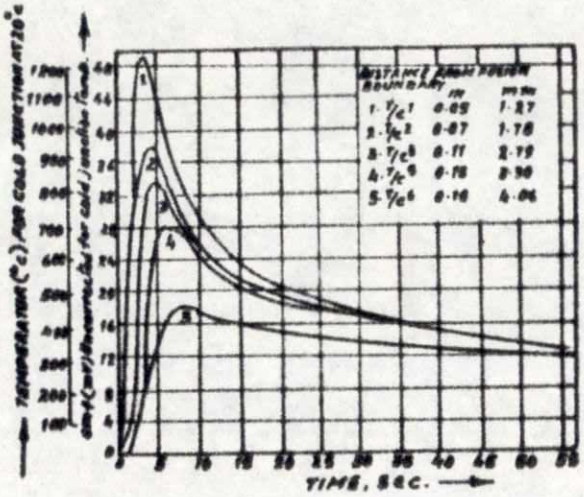

FIG. 2. EXPERIMENTALLY DETERMINED THERMAL CYCLES. (3)

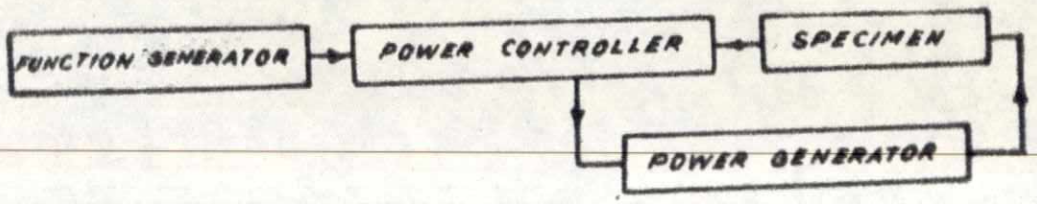

FIG. 3. FUNCTIONAL LAYOUT OF A CLOSED LOOP THERMAL SIMULATOR (7)

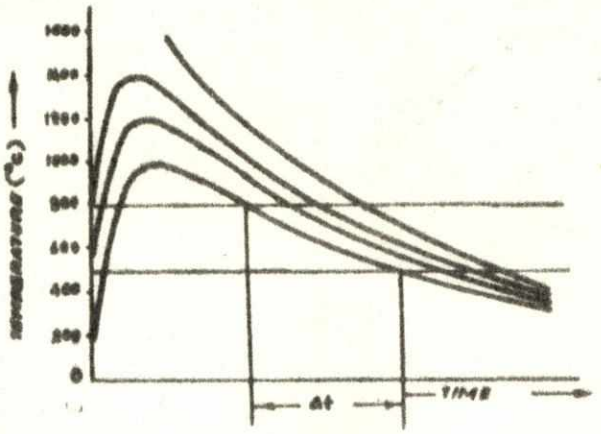

FIG. 4. SOME TEMP-TIME CURVES FOR SPOTS IN THE HEAT AFFECTED ZONE OF A WELD, AND DEFINITION OF Δt AS THE TIME REQUIRED FOR COOLING FROM 800°C TO 500°C. (4)

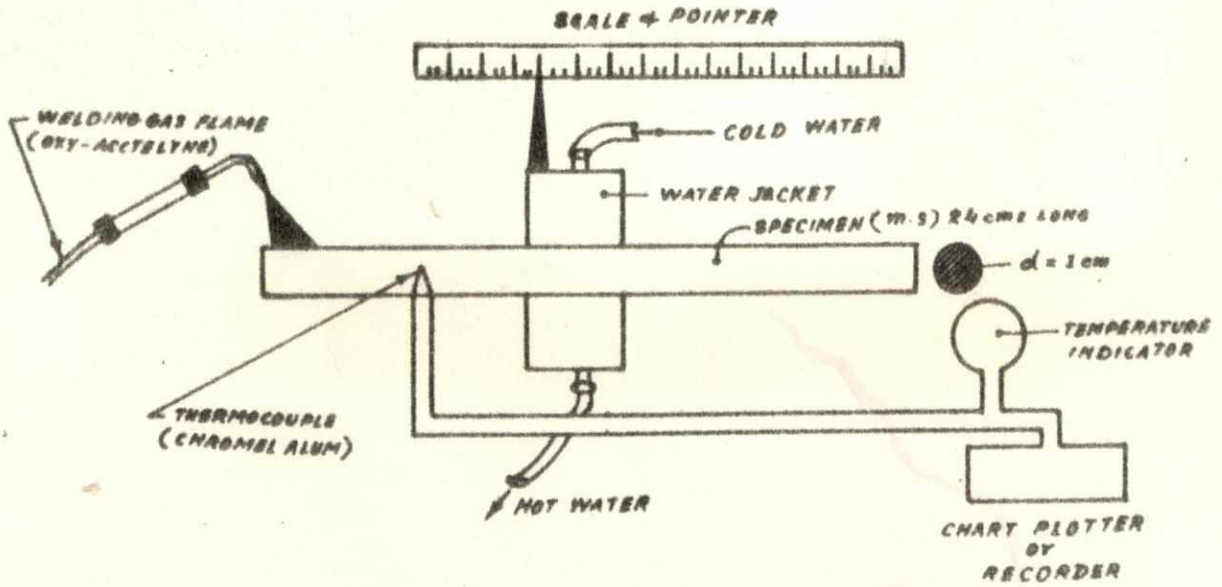

FIG. 5a. SCHEMATIC DIAGRAM OF THE EXPERIMENTAL SET UP

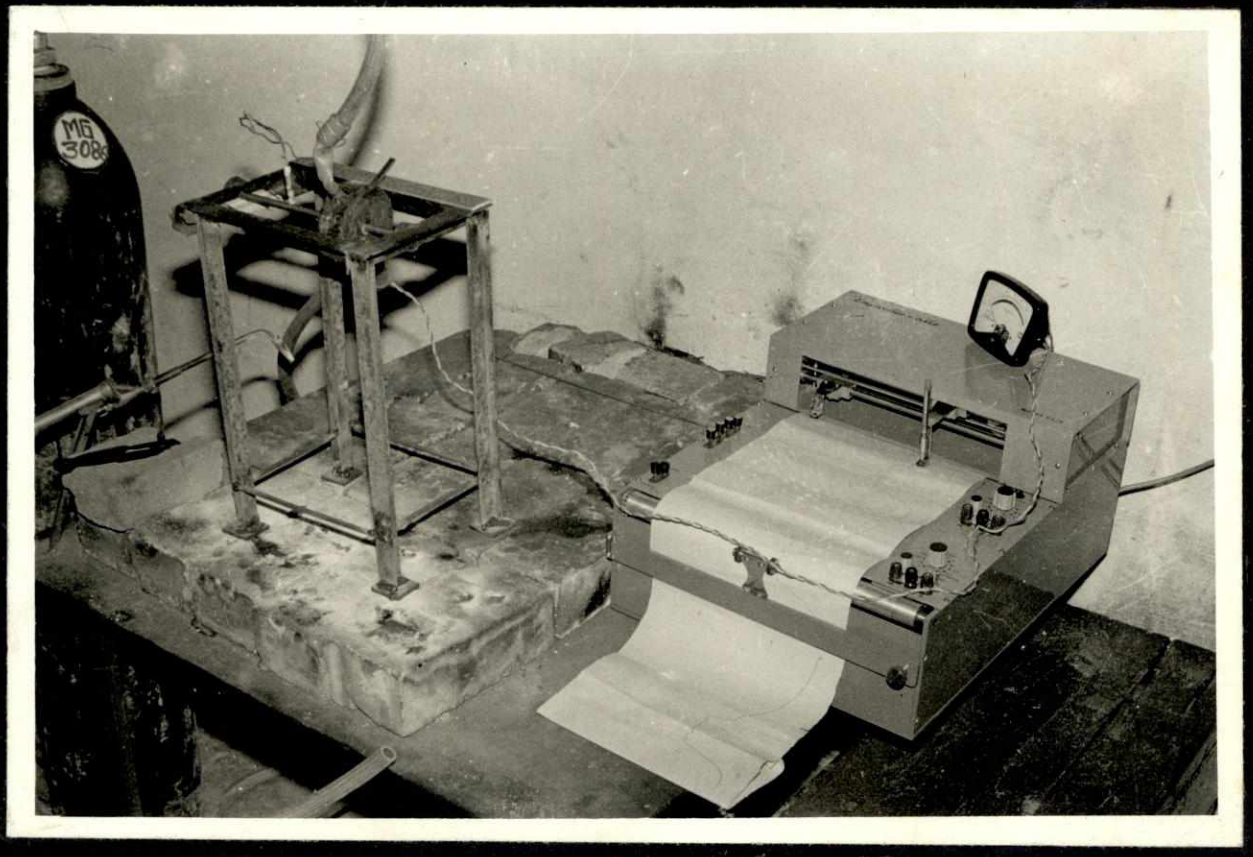

Fig. 5b : PICTORIAL VIEW OF EXPERIMENTAL SET UP

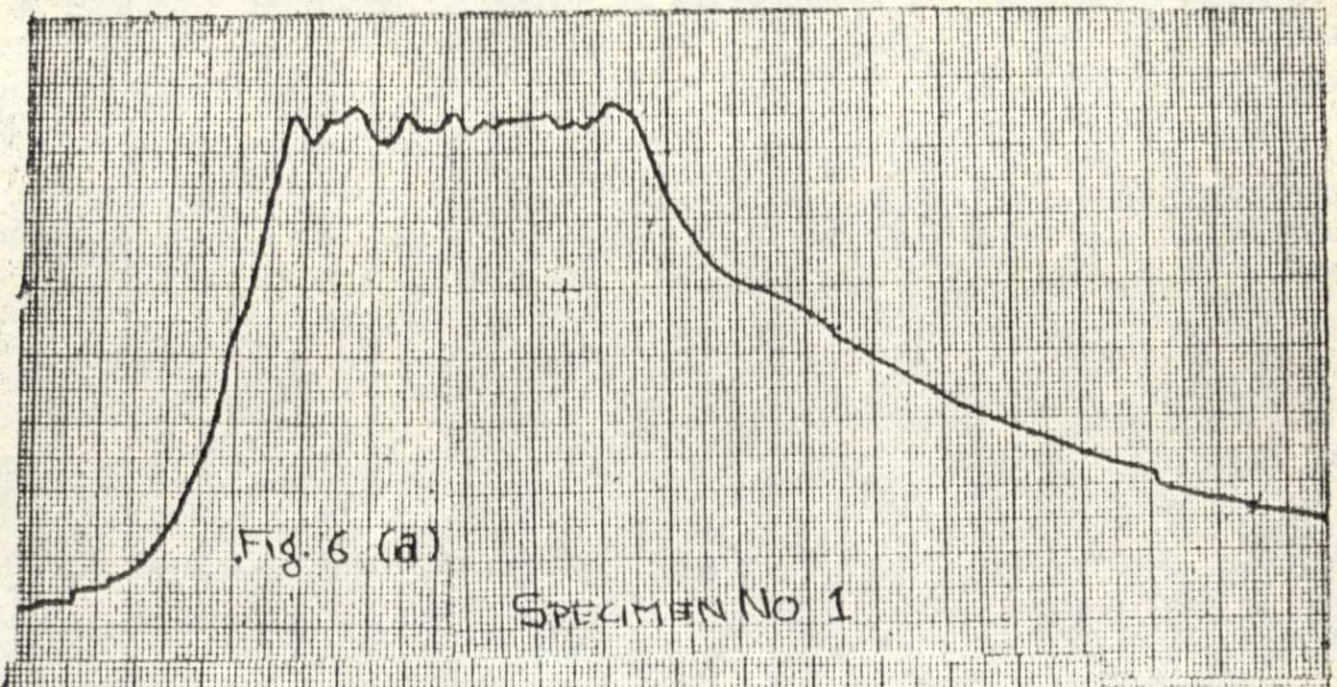

FIG. (6a,b) THERMAL CYCLES OBTAINED BY THE EXPERIMENTAL SET UP

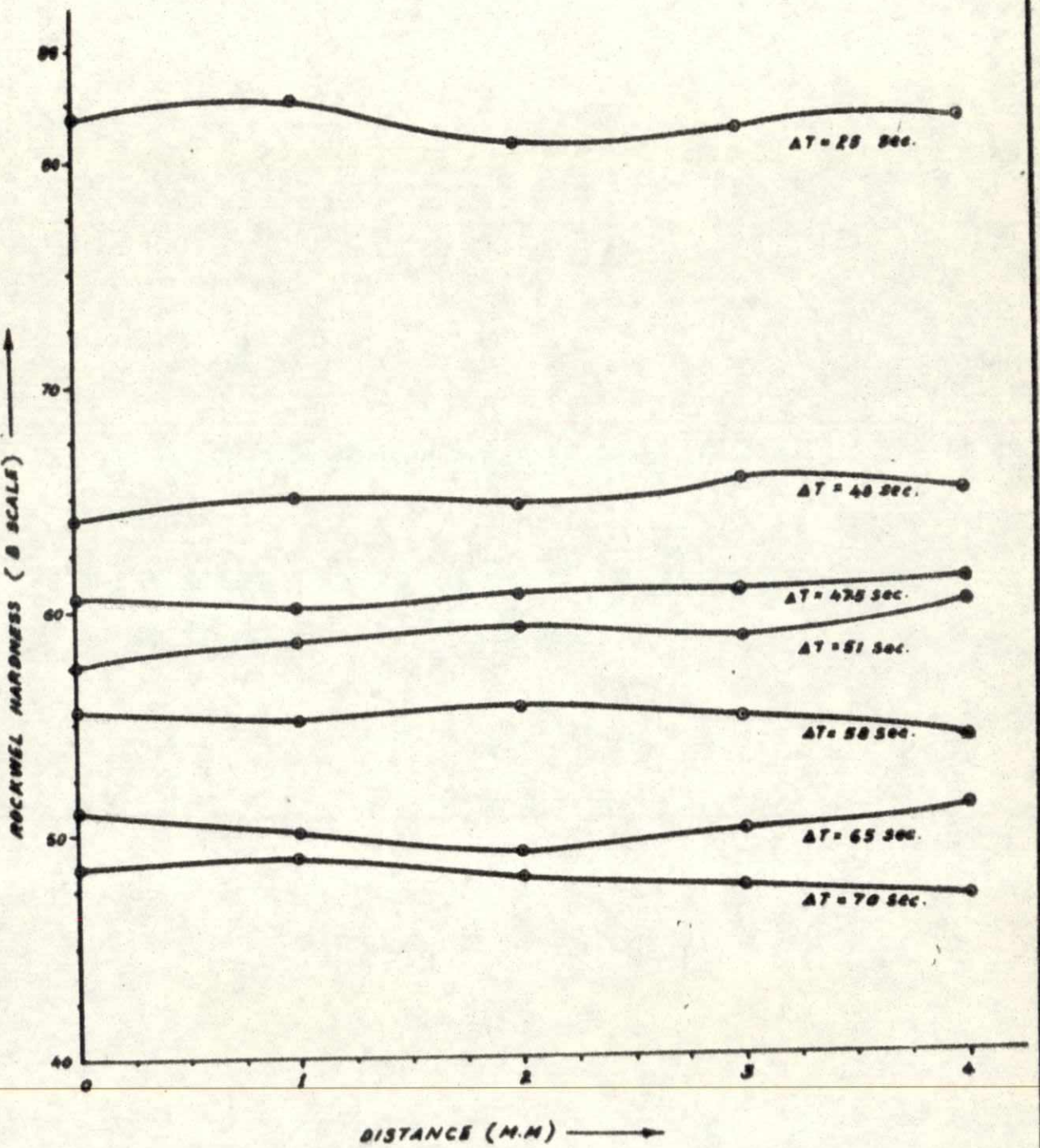

FIG. 7. HARDNESS OF VARIOUS SIMULATED SPECIMENS AT DIFFERENT COOLING RATES IN RADIAL DIRECTION.

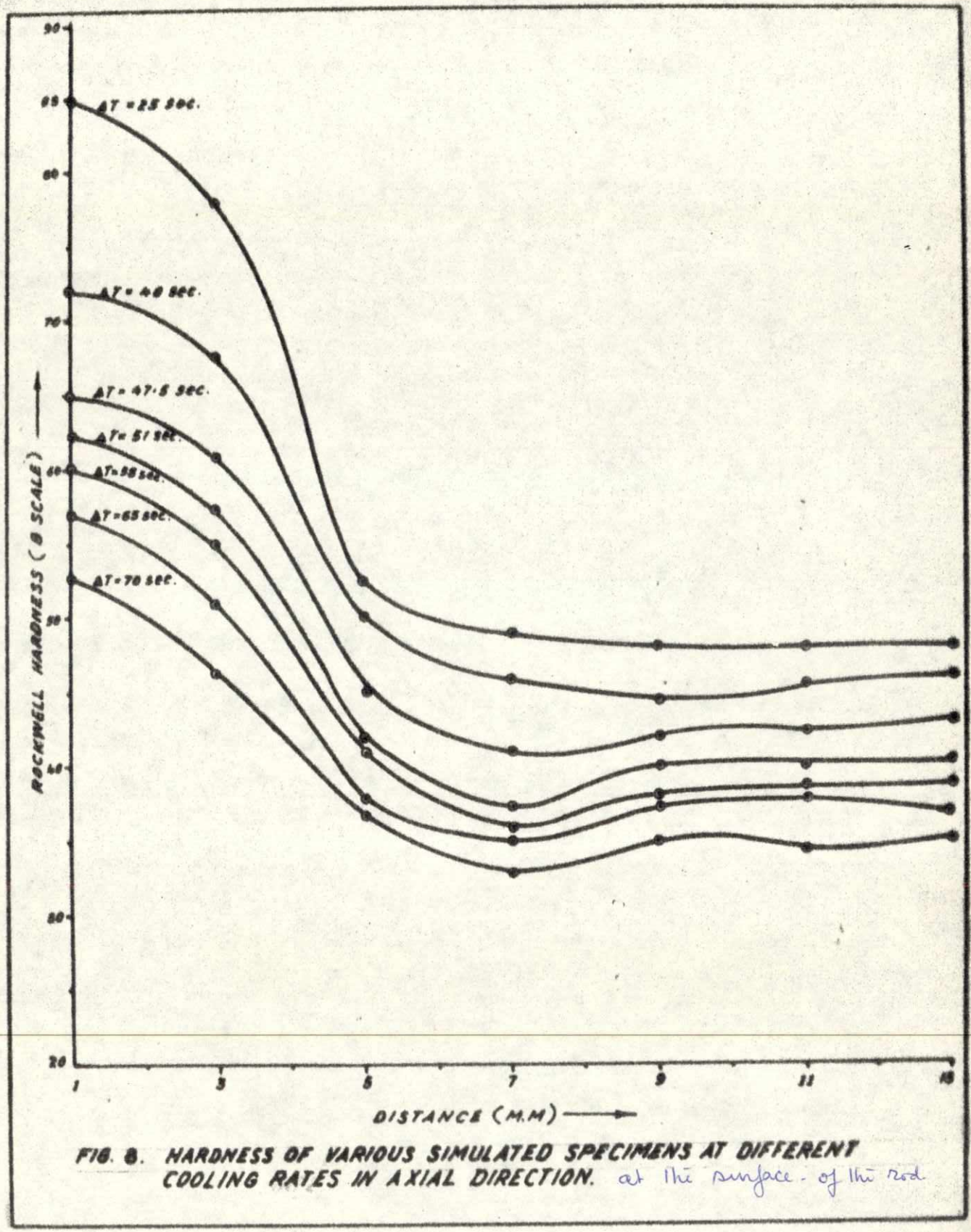

FIG. 8. HARDNESS OF VARIOUS SIMULATED SPECIMENS AT DIFFERENT COOLING RATES IN AXIAL DIRECTION. at the surface of the rod

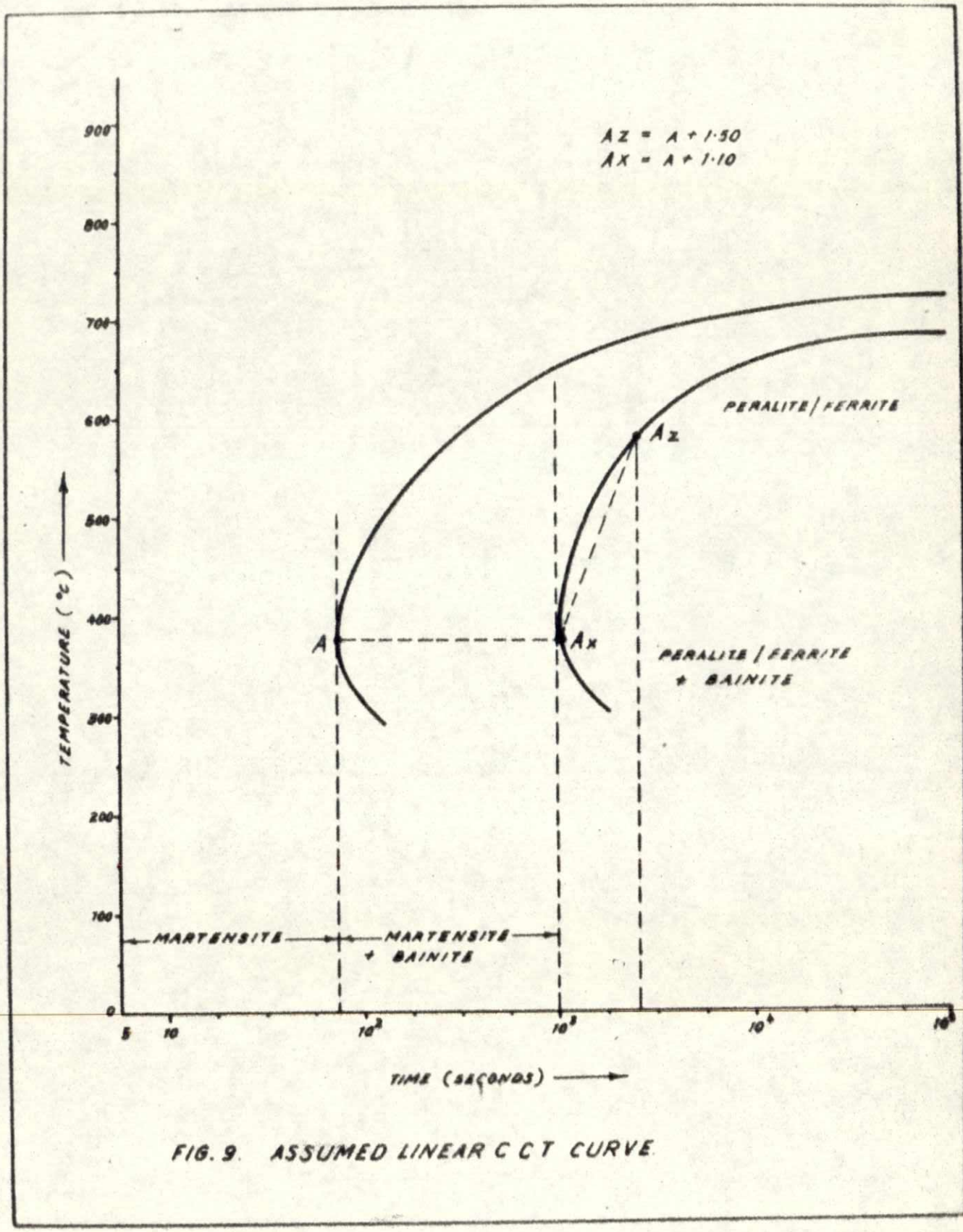

FIG. 9. ASSUMED LINEAR C C T CURVE

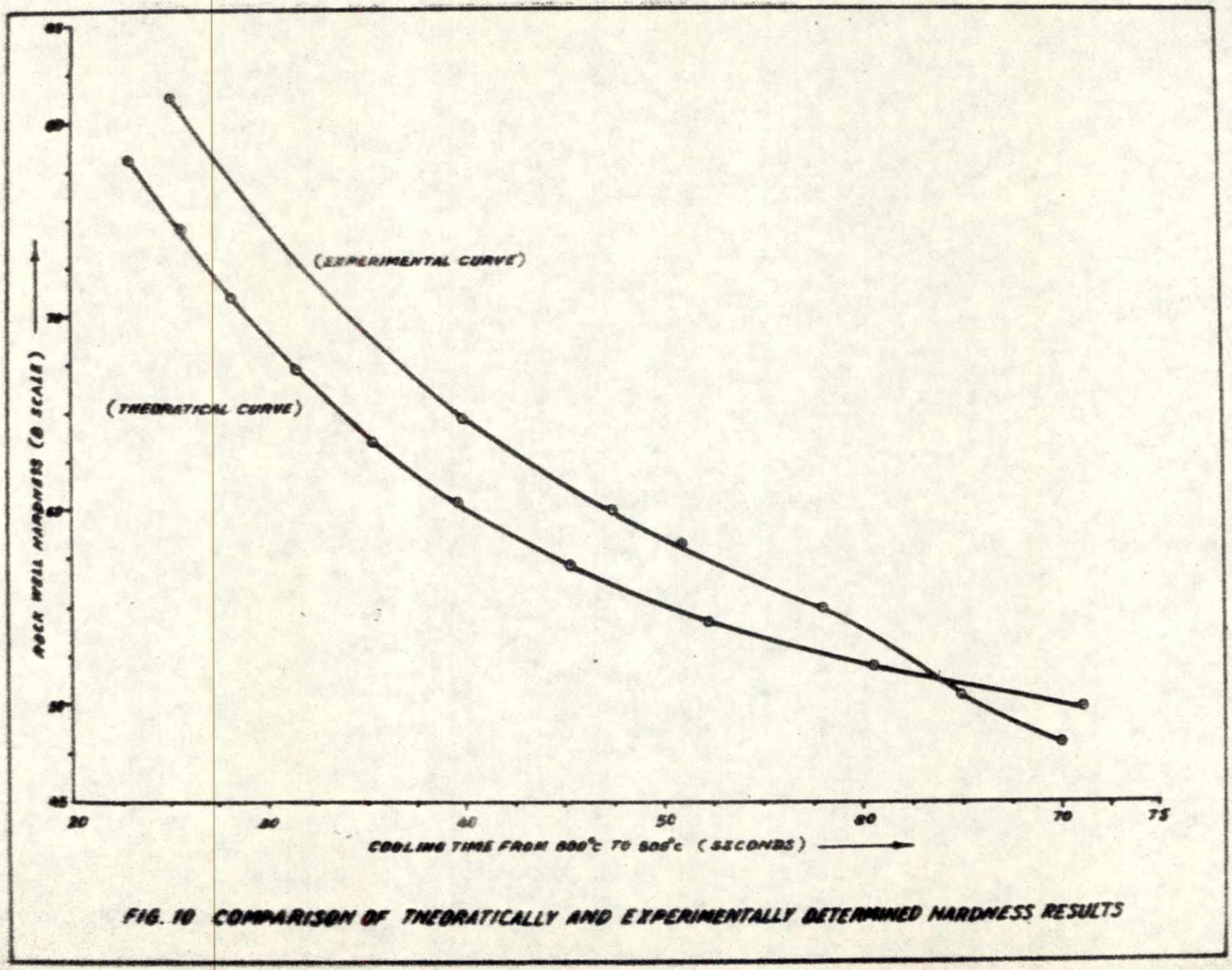

FIG. 10 COMPARISON OF THEORATICALLY AND EXPERIMENTALLY DETERMINED HARDNESS RESULTS

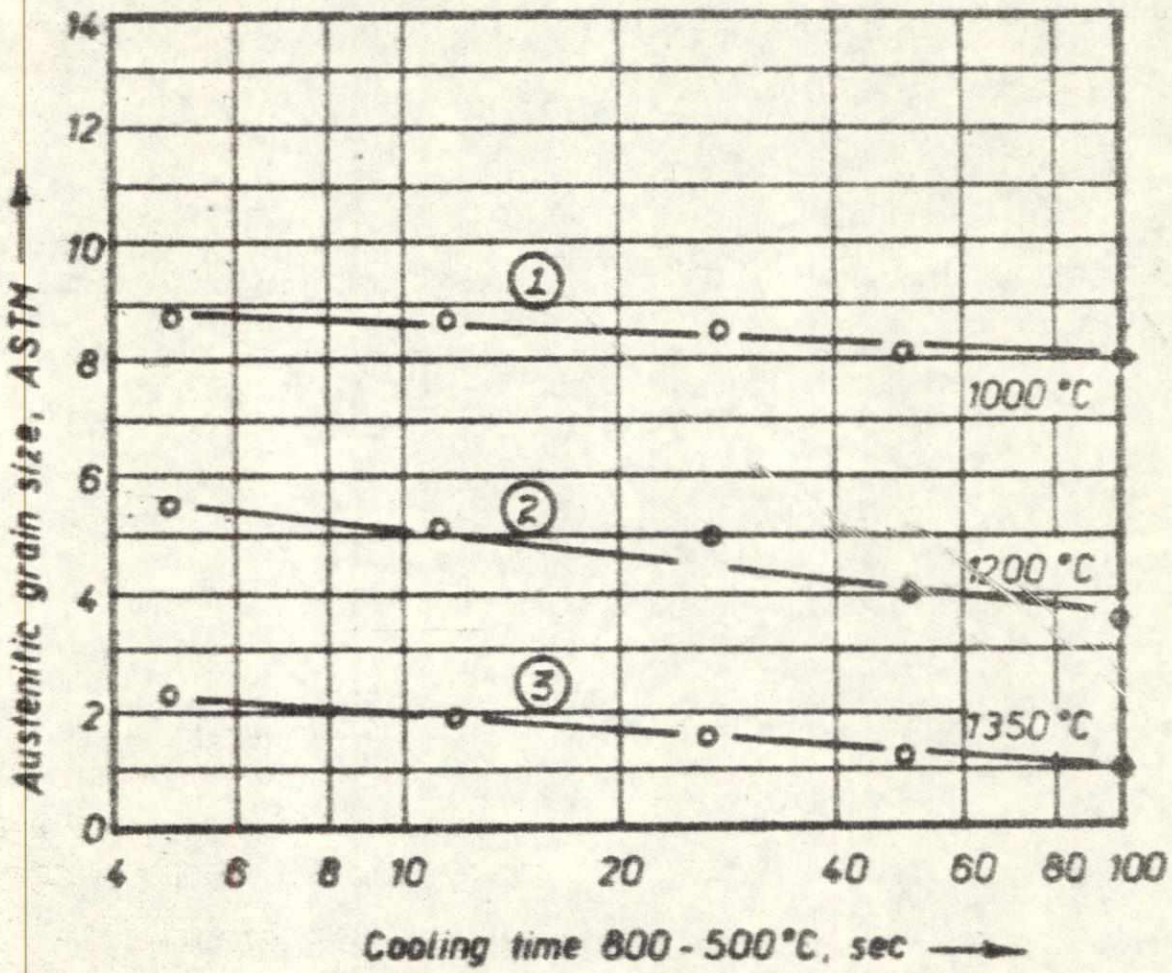

Fig. 11. Austenitic grain size as a function of cooling time 800-500°C at different peak temperatures

(reference.)

linearity ?

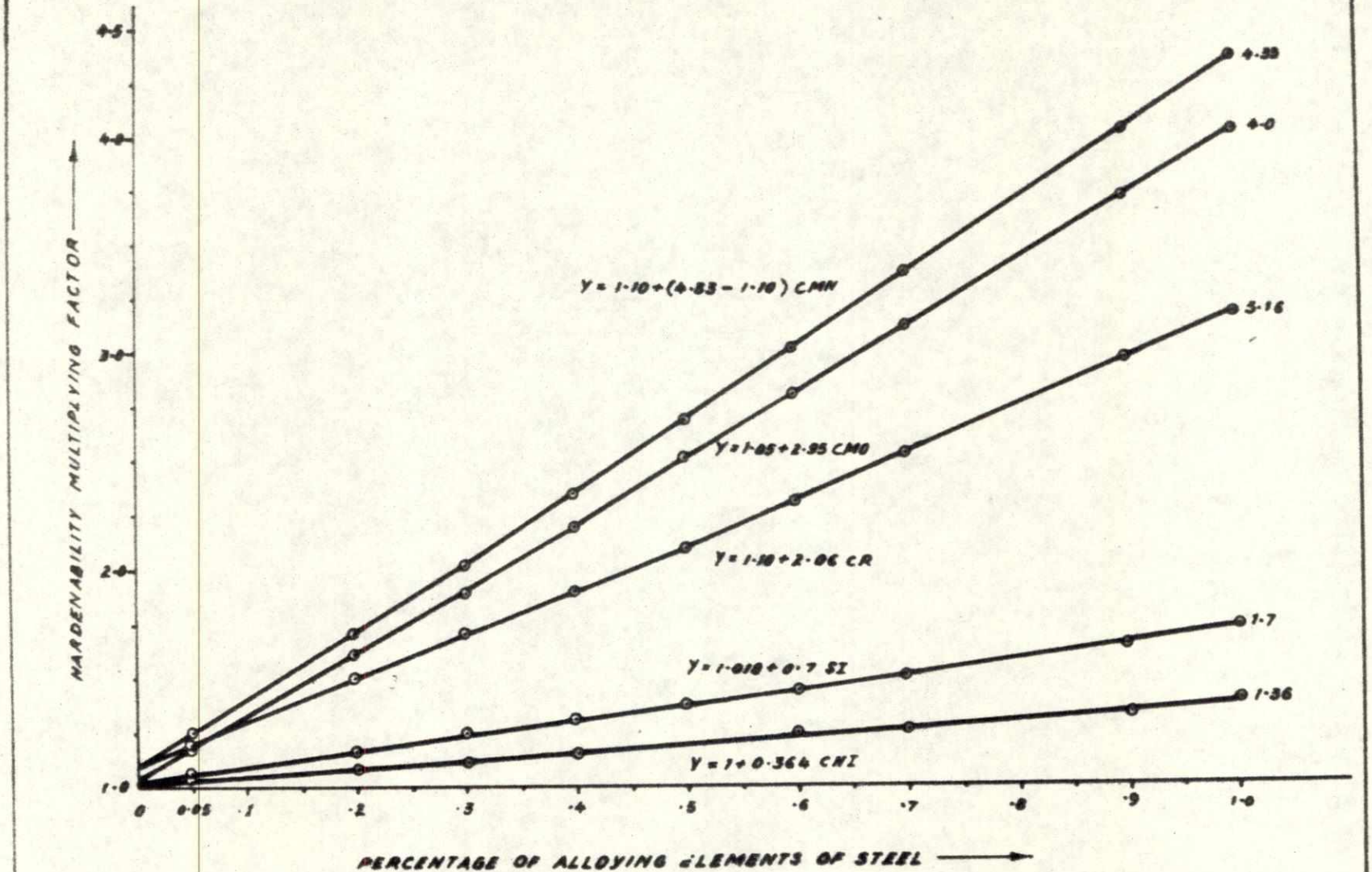

FIG. 12. HARDENABILITY MULTIPLYING FACTOR AT DIFFERENT PERCENTAGE OF VARIOUS ALLOYING ELEMENTS OF STEEL.

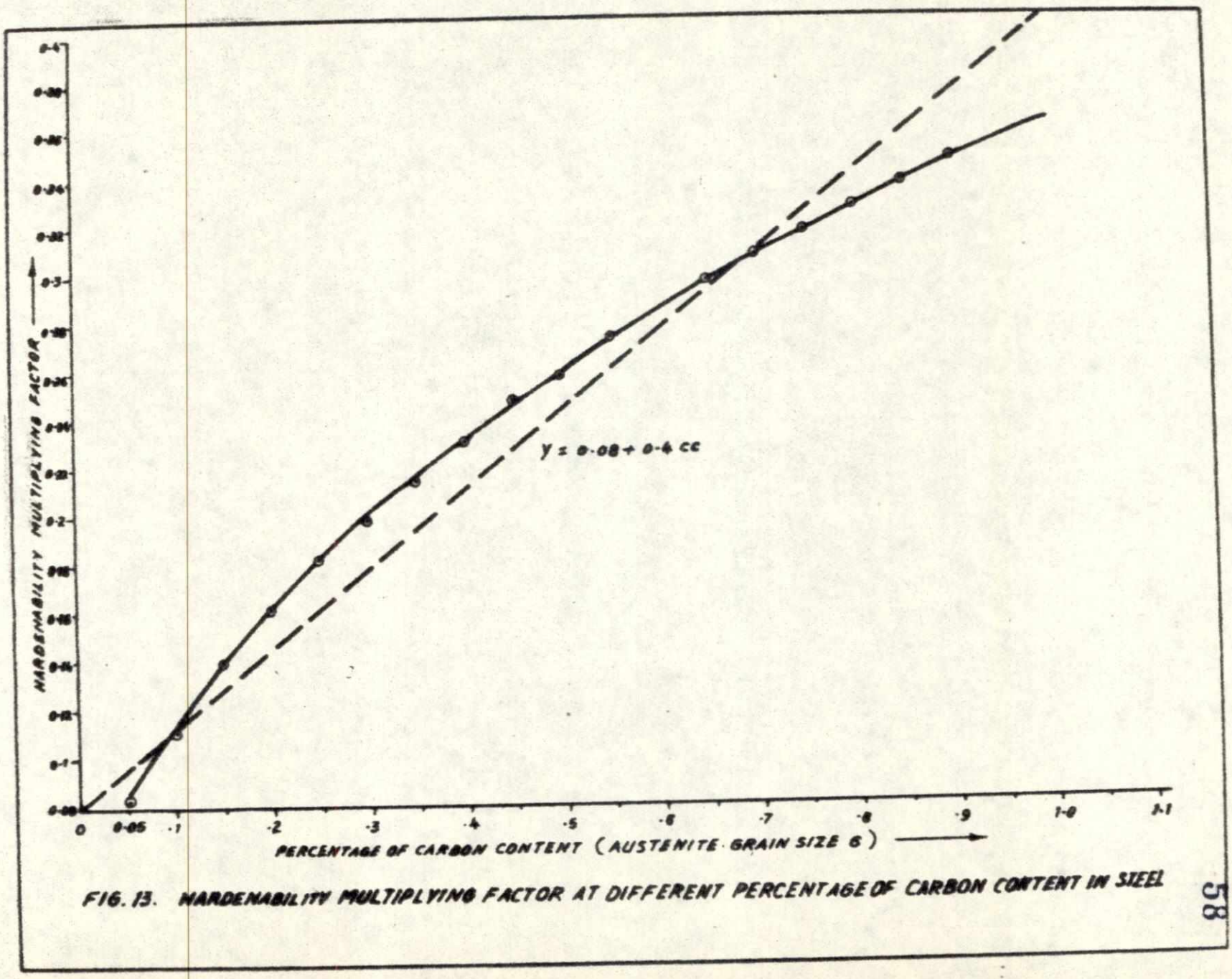

FIG. 13. HARDENABILITY MULTIPLYING FACTOR AT DIFFERENT PERCENTAGE OF CARBON CONTENT IN STEEL

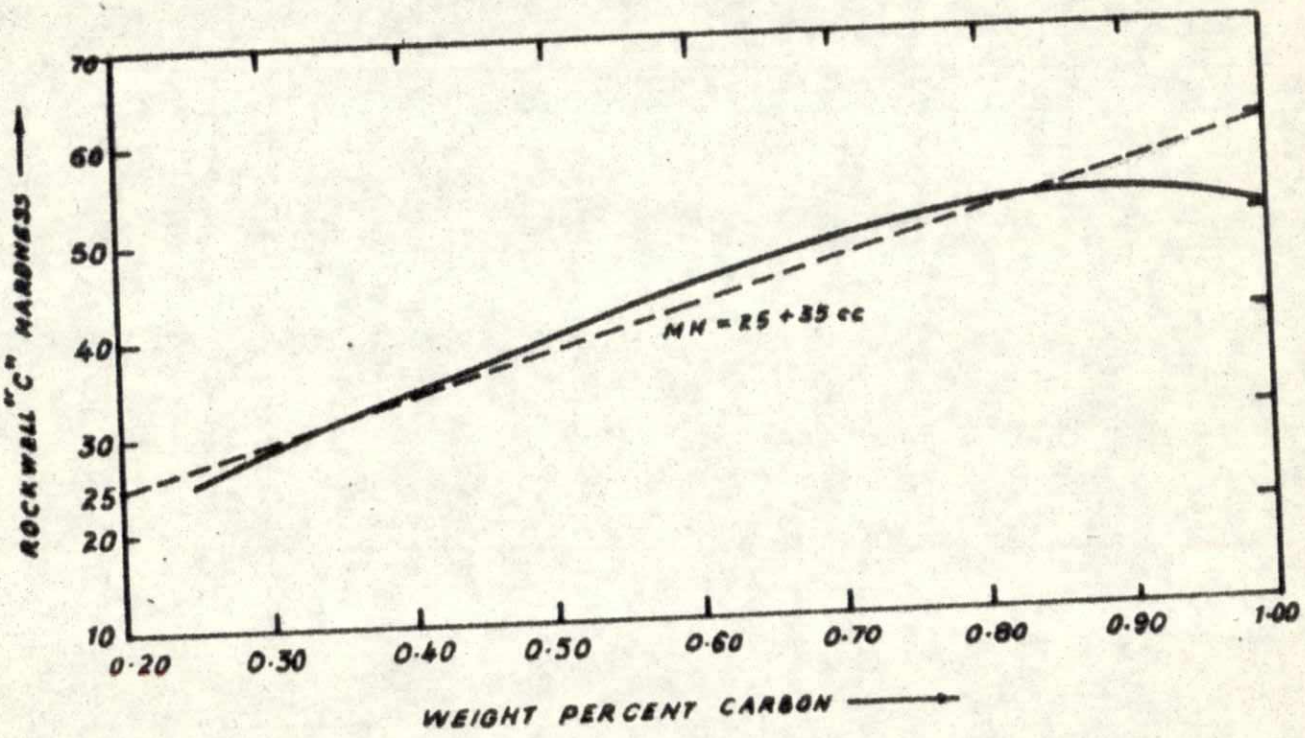

FIG.14 AVERAGE HARDNESS OF 50 PERCENT MARTESITE STRUCTURES IN LOW ALLOY STEEL (14, P 729)

FLOW DIAGRAM OF COMPUTER PROGRAMME

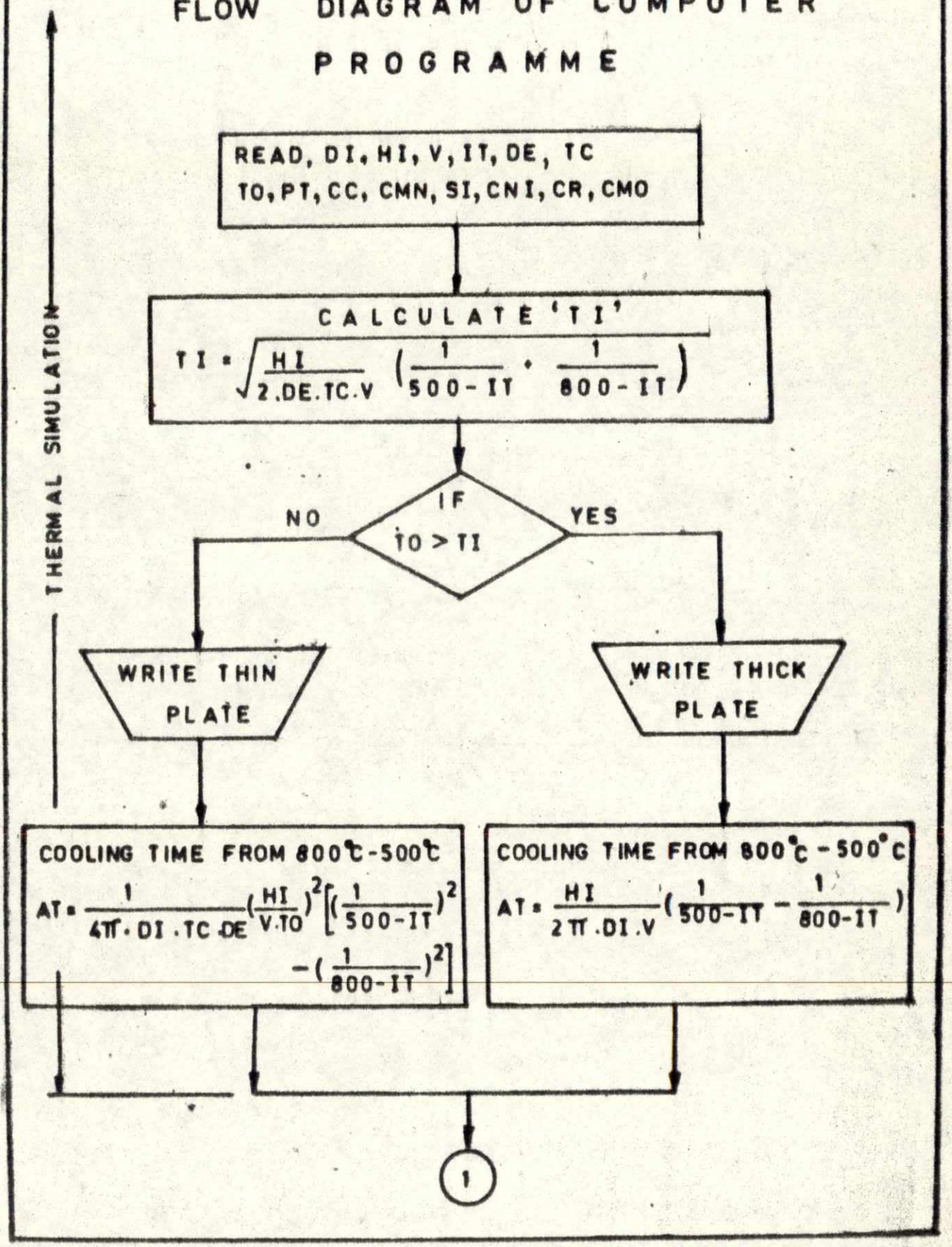

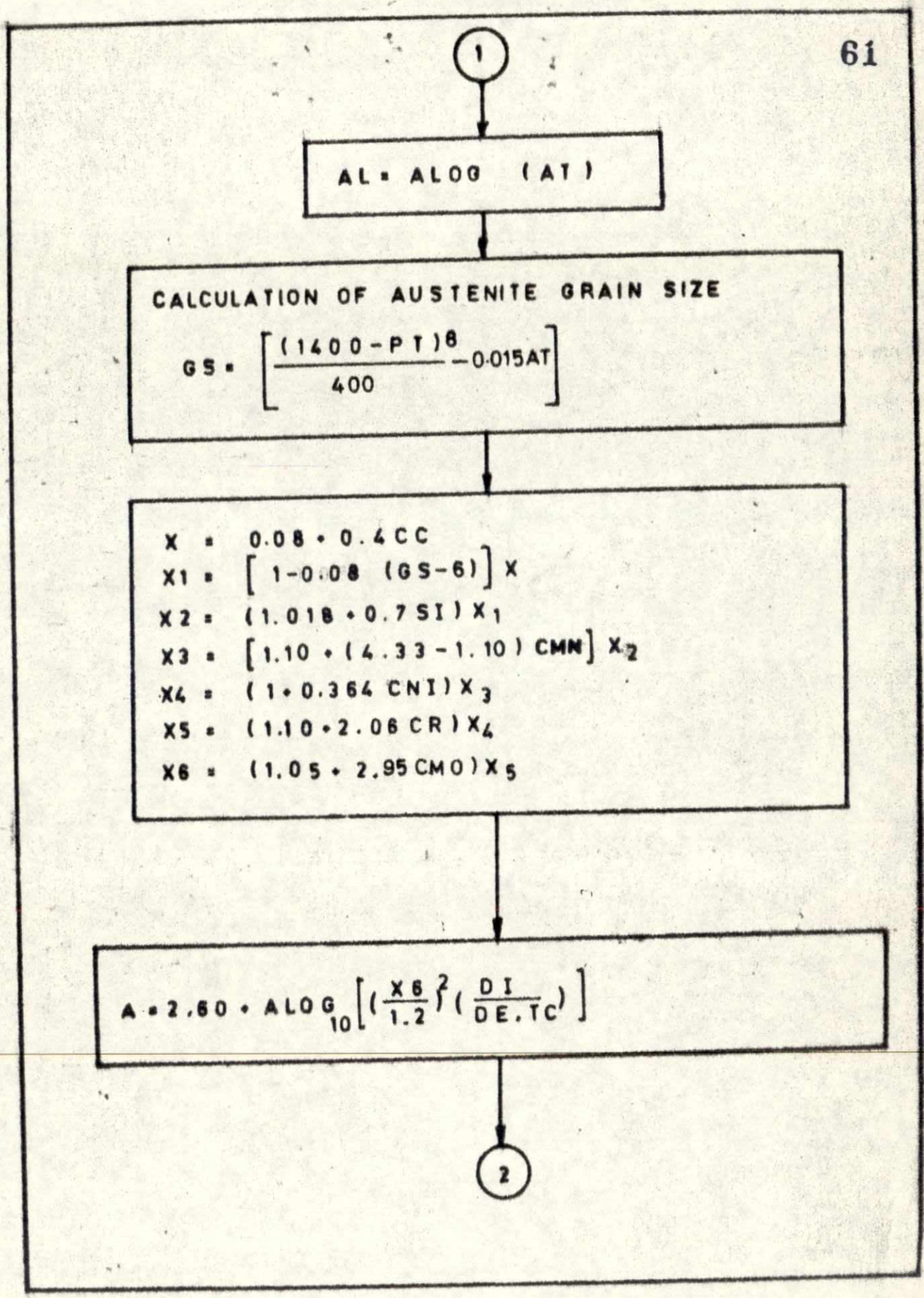
1
AL = ALOG (AT)
CALCULATION OF AUSTENITE GRAIN SIZE
GS = [(1400 - PT)^8 / 400 - 0.015AT]
X = 0.08 + 0.4CC
X1 = [1 - 0.08 (GS - 6)] X
X2 = (1.018 + 0.7 SI) X1
X3 = [1.10 + (4.33 - 1.10) CMN] X2
X4 = (1 + 0.364 CNI) X3
X5 = (1.10 + 2.06 CR) X4
X6 = (1.05 + 2.95 CMO) X5
A = 2.60 + ALOG10 [(X6 / 1.2)^2 (DI / DE.TC)]
2

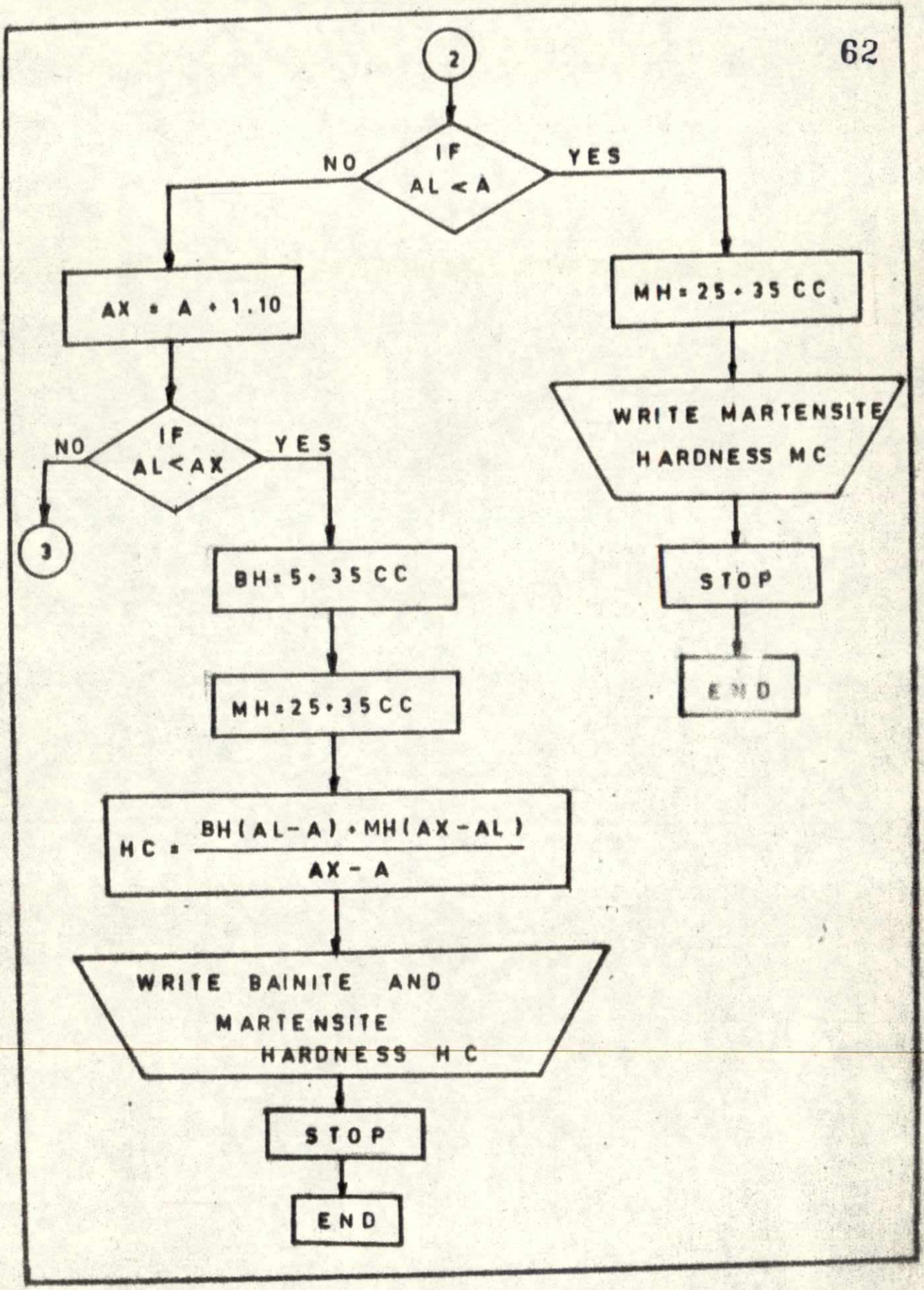
2
IF
AL < A
NO
YES
AX = A + 1.10
MH = 25 + 35 CC
WRITE MARTENSITE
HARDNESS MC
IF
AL < AX
NO
YES
3
BH = 5 + 35 CC
STOP
MH = 25 + 35 CC
END
HC = BH(AL-A) + MH(AX-AL) / AX - A
WRITE BAINITE AND
MARTENSITE
HARDNESS HC
STOP
END

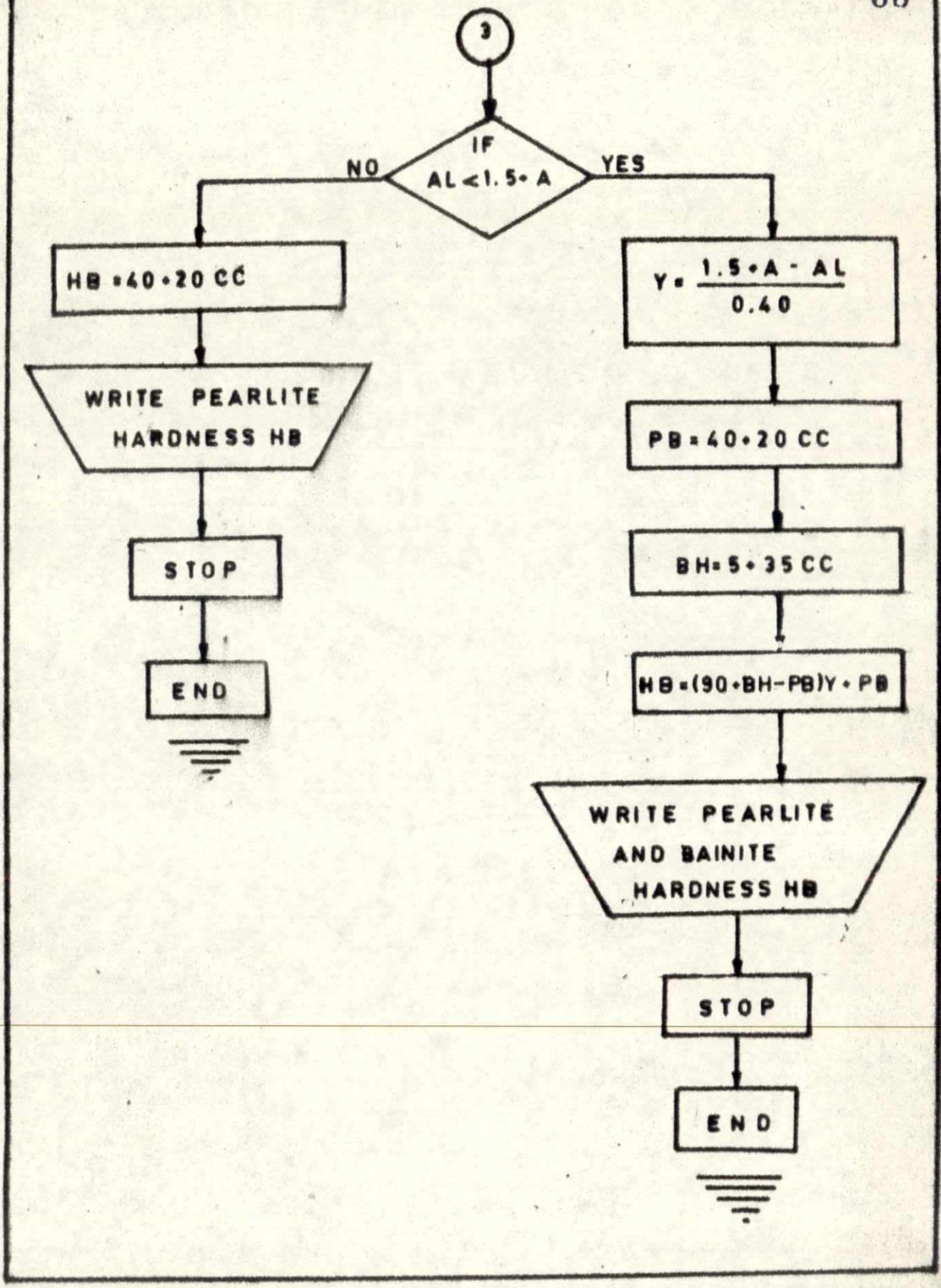
3
IF
AL<1.5*A
NO
YES
HB=40+20 CC
WRITE PEARLITE HARDNESS HB
STOP
END
Y=(1.5*A-AL)/0.40
PB=40+20 CC
BH=5+35 CC
HB=(90+BH-PB)Y+PB
WRITE PEARLITE AND BAINITE HARDNESS HB
STOP
END

```
                    THIN PLATE
                    AUSTENITE GRAIN SIZE
AGS=  10.94641 ASTM
 71.03679     .14000
PEARLITE AND BAINITE HARDNESS  49.9009 RB
```

```
                    THIN PLATE
                    AUSTENITE GRAIN SIZE
AGS=  11.10403 ASTM
 60.52838     .14000
PEARLITE AND BAINITE HARDNESS  51.9254 RB
                    THIN PLATE
                    AUSTENITE GRAIN SIZE
AGS=  11.22910 ASTM
 52.19029     .14000
PEARLITE AND BAINITE HARDNESS  54.4665 RB
                    THIN PLATE
                    AUSTENITE GRAIN SIZE
AGS=  11.33000 ASTM
 45.46354     .14000
PEARLITE AND BAINITE HARDNESS  57.3858 RB
                    THIN PLATE
                    AUSTENITE GRAIN SIZE
AGS=  11.41258 ASTM
 39.95819     .14000
PEARLITE AND BAINITE HARDNESS  60.5773 RB
                    THIN PLATE
                    AUSTENITE GRAIN SIZE
AGS=  11.48102 ASTM
 35.39549     .14000
PEARLITE AND BAINITE HARDNESS  63.9607 RB
                    THIN PLATE
                    AUSTENITE GRAIN SIZE
AGS=  11.53838 ASTM
 31.57190     .14000
PEARLITE AND BAINITE HARDNESS  67.4747 RB
                    THIN PLATE
                    AUSTENITE GRAIN SIZE
AGS=  11.58692 ASTM
 28.33600     .14000
PEARLITE AND BAINITE HARDNESS  71.0718 RB
                    THIN PLATE
                    AUSTENITE GRAIN SIZE
AGS=  11.62836 ASTM
 25.57324     .14000
PEARLITE AND BAINITE HARDNESS  74.7164 RB
                    THIN PLATE
                    AUSTENITE GRAIN SIZE
AGS=  11.66402 ASTM
 23.19568     .14000
PEARLITE AND BAINITE HARDNESS  78.3805 RB
N                              :          1
```